AD-A104 019   NAVAL OCEAN SYSTEMS CENTER SAN DIEGO CA   F/6 17/2
                SIGNALING TECHNIQUES FOR UNDERWATER ACOUSTIC COMMUNICATIONS, TO--ETC(U)
                JUN 81   L E HOFF
UNCLASSIFIED   NOSC/TR-649   NL

1 OF 1
AD A
104019

NOSC

END
DATE
FILMED
10-81
DTIC

AD A104019

LEVEL II ⑫

NOSC

DTIC
S ELECTE
SEP 1 0 1981
E

Technical Report 649

SIGNALING TECHNIQUES FOR UNDERWATER ACOUSTIC COMMUNICATIONS
Tonal and spread spectrum frequency shift key systems are compared

LE Hoff

6 June 1981

Final Report for Period October 1979—October 1980

DTIC FILE COPY

NAVAL OCEAN SYSTEMS CENTER
SAN DIEGO, CALIFORNIA 92152

81 9 10 027

ADMINISTRATIVE INFORMATION

ACKNOWLEDGMENTS

METRIC CONVERSION

To convert from	to	Multiply by
nautical miles	km	~ 1.85
miles	km	~ 1.61

REPORT DOCUMENTATION PAGE		READ INSTRUCTIONS BEFORE COMPLETING FORM
1. REPORT NUMBER NOSC Technical Report 649 (TR 649)	2. GOVT ACCESSION NO.	3. RECIPIENT'S CATALOG NUMBER
4. TITLE (and Subtitle) SIGNALING TECHNIQUES FOR UNDERWATER ACOUSTIC COMMUNICATIONS Tonal and spread spectrum frequency shift key systems are compared		5. TYPE OF REPORT & PERIOD COVERED Final October 1979 – October 1980
		6. PERFORMING ORG. REPORT NUMBER
7. AUTHOR(s) LE Hoff		8. CONTRACT OR GRANT NUMBER(s)
9. PERFORMING ORGANIZATION NAME AND ADDRESS Naval Ocean Systems Center San Diego, CA 92152		10. PROGRAM ELEMENT, PROJECT, TASK AREA & WORK UNIT NUMBERS PE 61152N ZR0110815
11. CONTROLLING OFFICE NAME AND ADDRESS		12. REPORT DATE 6 June 1981
		13. NUMBER OF PAGES 44
14. MONITORING AGENCY NAME & ADDRESS(if different from Controlling Office)		15. SECURITY CLASS. (of this report) Unclassified
		15a. DECLASSIFICATION/DOWNGRADING SCHEDULE
16. DISTRIBUTION STATEMENT (of this Report) Approved for public release; distribution unlimited		
17. DISTRIBUTION STATEMENT (of the abstract entered in Block 20, if different from Report)		
18. SUPPLEMENTARY NOTES		

19. KEY WORDS (Continue on reverse side if necessary and identify by block number)

Underwater acoustics	Frequency shift
Underwater communications	Fading (acoustic waves)
Tonal pulses	Distortion
Spread spectrum	RAKE
Multipath transmission	

20. ABSTRACT (Continue on reverse side if necessary and identify by block number)

This study compares two sophisticated signaling schemes to compensate for distortions in underwater acoustic channels, where the channel rate of change approaches the reciprocal of the multipath time spread. The first scheme uses tonal pulses much longer than the channel multipath spread. The second (commonly called RAKE) uses spread spectrum pulses to resolve the multipath and an adaptive receiver to combine the multipath echoes coherently. Analysis shows that the RAKE scheme (1) performs considerably better for slowly fading channels and (2) can use a smaller decision interval and can therefore tolerate higher fade rates.

EXECUTIVE SUMMARY

The underwater acoustic channel can provide important communication links for Navy C^3. It is, however, degraded by severe multipath dispersion, Doppler shifts, and fading, all of which seriously distort the transmitted signal. Channel distortions can cause excessively high error rates unless sophisticated signaling schemes are used. Two schemes are considered. The first minimizes channel distortions by using tonal pulses much longer than the channel multipath spread. The second (commonly called RAKE) uses spread spectrum pulses to resolve the multipath and an adaptive receiver to combine the multipath echoes coherently. This study compares the merits of these two schemes for acoustic channels, where the channel rate of change approaches the reciprocal of the multipath time spread.

High frequency (hf) channels and underwater acoustic channels have similarities; historically, researchers have shared signal processing concepts. At the initiation of this NOSC IR/IED task, it was felt that the background of the investigators in the area of hf communication would provide a useful perspective.

During FY80, narrowband and wideband models were derived that describe signals propagating through an underwater acoustic channel. They are based upon a stochastic, time-variant filter. The narrowband model is similar to models developed for hf, but the wideband model is quite different because of the effects of Doppler on the channel correlation bandwidth and the signal envelope compression or expansion.

The mathematical results of Bello and Nelin on tonal FSK and the results of Hoff on RAKE were used in evaluating the two signaling schemes. These works were based on channel models that exhibit small Doppler shifts, which cause negligible pulse stretching or compression. Analysis shows that channel time variance causes an irreducible error bound for both signaling schemes. The maximum channel frequency spread that can be tolerated is different for the two schemes and depends upon the receiver decision time interval. The RAKE scheme can use a smaller decision interval and can therefore tolerate higher fade rates than the tonal scheme. For slowly fading channels, the tonal scheme performs considerably poorer than the RAKE scheme. For example, if three multipaths are present, the tonal system requires a signal to noise ratio (SNR) about 23 dB greater than that required by the RAKE system to achieve a 10^{-4} bit error rate.

These results were based upon analysis of channels where Doppler is a minor problem. It is recommended that this work be extended to acoustic channels with severe Doppler. Because of the large improvement indicated by the analysis, the problem warrants further research.

Accession For	
NTIS GRA&I	☒
DTIC TAB	☐
Unannounced	☐
Justification	

By	
Distribution/	
Availability Codes	
Dist	Avail and/or Special
A	

1

CONTENTS

1. INTRODUCTION

BACKGROUND

Communication to submarines at depth is a problem of continuing interest to the Navy. Although there are problems with achieving continuous coverage, it is possible to provide acoustic signals with good SNR at considerable depth and range. Thus, underwater acoustic propagation has the potential to provide communications with submarines.

The acoustic channel, however, is degraded by severe multipath dispersion, Doppler shifts, and fading, which seriously distort the transmitted signal. The distortions can cause excessively high error rates unless sophisticated signaling schemes are used. In this report, two distinct classes of signaling schemes are considered for underwater acoustic communications. The first, a traditional approach, uses long tonal pulses to send digital information. The effects of channel fading on error rate are minimized by incoherent techniques, such as diversity and/or error detection and correction coding. The second uses wideband spread spectrum pulses to send digital information. The effects of channel fading and distortions are minimized by using adaptive filtering at the receiver to combine channel multipaths coherently. This technique is commonly called RAKE.

This NOSC IR/IED study, which compared the merits of these two signaling schemes for acoustic channels, consisted of the following: Determine a realistic and tractable model for the overspread underwater acoustic channel, and compare the performance of RAKE and tonal FSK with respect to probability of error on the overspread underwater acoustic channel.

APPROACH

The investigators of this study have a background in the area of hf radio communications (2–32 MHz). The hf channel is a classic example of a multipath dispersive channel. The hf and underwater acoustic channels have similarities; historically, researchers have shared technological ideas. At the initiation of this NOSC IR/IED task it was felt that because of their background, the investigators would have a useful perspective for comparing tonal and spread spectrum signaling.

In section 2 we develop a mathematical model for the underwater acoustic channel and compare it with the hf channel. Doppler is the most significant feature of the acoustic channel model that is missing in the hf channel. Since Doppler shifts at hf are small compared to the signal bandwidth, they cause almost no envelope distortion. In the underwater acoustic channel, however, Doppler shifts and envelope distortions can be severe. We show that for small signal bandwidths and channel Doppler, the underwater acoustic channel model is similar to models used for the hf channel. Thus there exists a subset of underwater acoustic channels that are analogous to hf channels but have different scale factors for time and frequency.

Our approach to comparing the signaling schemes is to use error rate analysis developed for narrowband channels with small Doppler. The analysis incorporates all the features of the acoustic channel except the Doppler compression/expansion of the signal envelope. We felt that our approach would contribute to an understanding of the relative performance of the two techniques on highly time-variant channels and would provide a basis for extending the work to acoustic channels with severe Doppler distortion.

In section 3 we evaluate and compare the two signal processing schemes. First, we present the results of Bello and Nelin on tonal FSK (ref 1,2) and the results of Hoff (ref 3) on a signaling scheme similar to RAKE. The analysis treats the problems of time dispersion (T_L) and fading (B) separately. First, time-invariant channels with severe time dispersion, then channels with severe fade rates but fixed time dispersion are studied. The two techniques are compared for channels where the time dispersion is fixed but the channel fade rate (channel time variance) increases so that the product BT_L approaches unity.

Section 4 presents a summary, and section 5 gives recommendations for further work.

2. UNDERWATER ACOUSTIC CHANNEL

OVERVIEW

Acoustic propagation has several characteristics that make reliable underwater communications difficult to achieve. We discuss some of the characteristics in this section. Sound does not travel in a straight line but refracts (bends) as it passes through the ocean. The bending is caused by changes in sound velocity (c) with increasing depth. The speed of sound in seawater varies from about 1450 to about 1570 m/s. It increases with increasing temperature, salinity, and pressure. In the ocean, temperature is the primary variable, influenced by location, depth, and season.

Figure 1 shows three basic shapes of the sound-velocity profile (ref 4,5). Over much of the deep ocean area the temperature structure has three parts: (1) A relatively warm surface layer, often showing isothermal structure (a vertical profile). (2) The main thermocline, in which the temperature decreases rapidly with depth — the decrease in temperature dominates the increase in pressure, causing the speed of sound to decrease. (3) The cold water layers, in which the temperature decreases slowly with depth — the increase in pressure dominates, causing the speed of sound to increase. Part A represents this typical sound profile. Sound signals transmitted from a source S at a depth near the velocity minimum in part A are said to be in the sound fixing and ranging (sofar) channel. These signals propagate long distances, especially for frequencies below 500 Hz, because the path loss is small. The sofar channel is about 1000 m deep but tends to get shallower toward the poles.

The ray trace in part B is an example of a surface wave channel, where because of a temperature inversion the signal travels just under the surface of the ocean. Part C shows a sound profile typical of the arctic. As in part B, the ray path of the sound is bent upward, with the result that it bounces along the surface.

1. PA Bello and BD Nelin, The Effect of Frequency Selective Fading on the Binary Error Probabilities of Incoherent And Differentially Coherent Matched Filter Receivers, IEEE Transactions on Communication Systems, p 170-186, June 1963.

2. R Price and PE Green, Jr, Communication Techniques For Multipath Channels, Proceedings of the IRE, vol 46, p 555-570, March 1958.

3. LE Hoff, Probe Signaling on Fading Multipath Communication Channels, PhD thesis at the University of California, San Diego, 1979.

4. CB Officer, Sound Transmission, McGraw-Hill Book Company Inc, New York, 1958, chapter 4.

5. I Tolstoy and CS Clay, Ocean Acoustics, McGraw-Hill Book Company, New York, 1966, chapter 5.
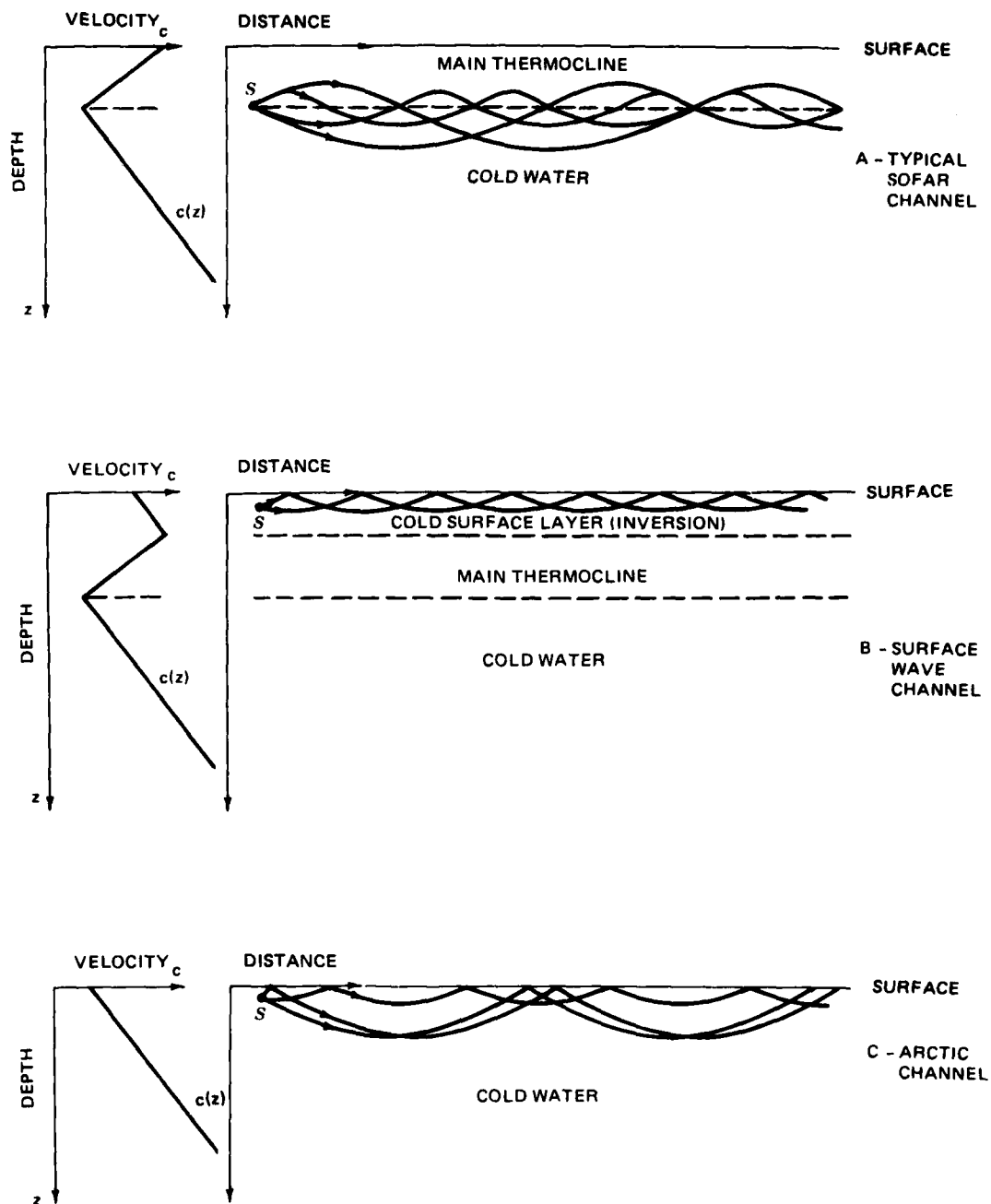
VELOCITY$_c$ DISTANCE

DEPTH

z

c(z)

SURFACE

MAIN THERMOCLINE

S

COLD WATER

A – TYPICAL SOFAR CHANNEL

VELOCITY$_c$ DISTANCE

DEPTH

z

c(z)

SURFACE

S

COLD SURFACE LAYER (INVERSION)

MAIN THERMOCLINE

COLD WATER

B – SURFACE WAVE CHANNEL

VELOCITY$_c$ DISTANCE

DEPTH

z

c(z)

SURFACE

S

C – ARCTIC CHANNEL

COLD WATER

Figure 1. Sound velocity profiles for deep water. [From Ocean Acoustics, by Tolstoy and Clay (ref 5). Copyright 1966 by McGraw-Hill, Inc. Used with the permission of McGraw-Hill Book Company.]

Although underwater acoustic propagation can enable communications out to 185 km (100 nmi) or more, continuous coverage is difficult to provide. Figure 2 shows sound intensity as a function of range (ref 5). Charges of TNT were detonated at 12-m depths, and the time integral of the square of the pressure (ie, the power) was recorded at 100-m depths. Note the nearly periodic 70- km convergence zones. Between the convergence zones, the sound power drops 15–30 dB. To achieve continuous coverage, the transmitter must provide enough power for reliable communications between the convergence zones. Alternatively, multisite transmissions may be used to fill in the regions between convergence zones.

The underwater acoustic channel is a time-variant multipath dispersive channel. Figure 3 shows a sound-velocity profile and a ray trace (ref 5). In this case, the sound is generated and received in the sofar channel, which occurs in the knee of the sound-velocity profile. Sound can take more than one path to the receiver, and each path can have a diffused path structure. Thus, transmitted pulses can be stretched by multipath, and sequences of information pulses can be distorted by intersymbol interference. Figures 4 and 5, taken from Urich (ref 6), exemplify a sofar signal. Figure 4 shows the explosive pulse, recorded near the source; figure 5 shows the envelope of the sound received at a distance from the source. The pulse has been stretched from a few milliseconds to several seconds. Unless the bit rate is extremely low (less than 0.1 bit/second), the communication system must be prepared to process signals with severe intersymbol interference.

The channel response changes very slowly in the sofar channel, but the channel may have significant Doppler shift with movement of one or both terminals.
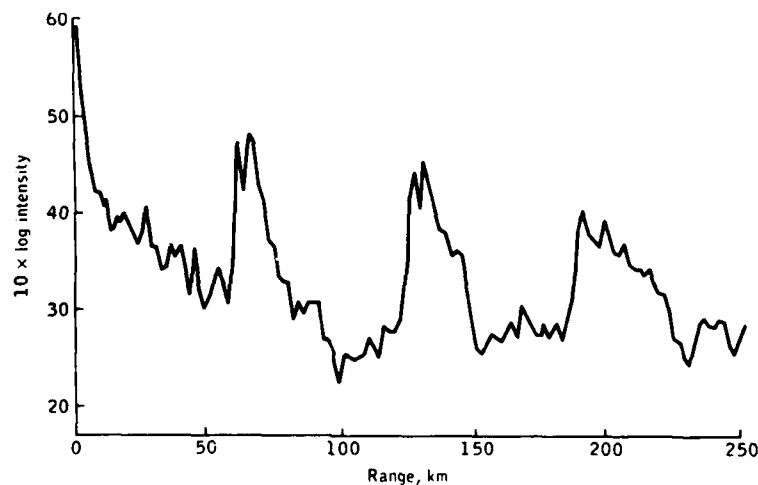

Figure 2. Observed convergence zones in a typical North Atlantic experiment. [From Ocean Acoustics, by Tolstoy and Clay (ref 5). Copyright 1966 by McGraw-Hill, Inc. Used with the permission of McGraw-Hill Book Company.]

6. RJ Urich, Multipath Propagation and Its Effects on Sonar Design and Performance in the Real Ocean, paper in Aspects of Signal Processing, Part I, edited by G Taccone, D Reidel Publishing Company, 1977.
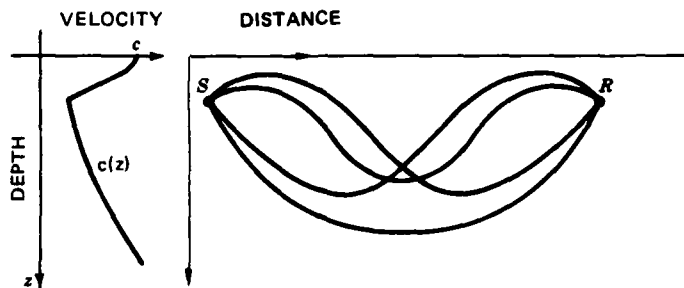
6

Figure 3. Ray paths for a sofar channel. [From Ocean Acoustics, By Tolstoy and Clay (ref 5). Copyright 1966 by McGraw-Hill, Inc. Used with permission of McGraw-Hill Book Company.]
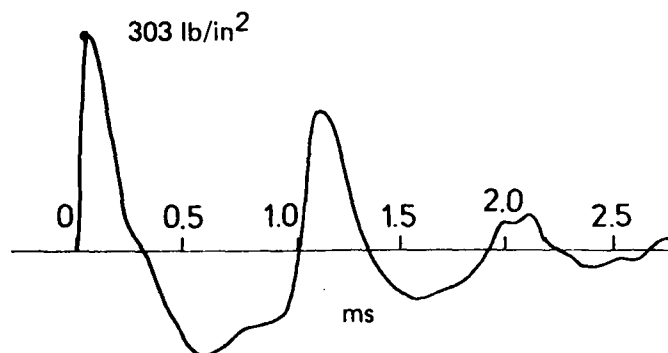

Figure 4. Pressure signature of a 1-pound charge detonated at 22 000 feet and recorded overhead at a shallow depth. (From ref 6. Reprinted by permission of D Reidel Publishing Company, Dordrecht - Holland.)
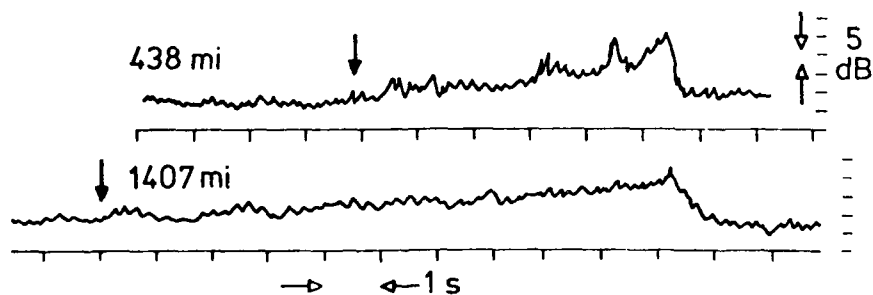

Figure 5. Envelope of an explosive pulse after traveling through the deep ocean (sofar) sound channel. The solid arrows show the approximate times of commencement of the received signal (From ref 6. Reprinted by permission of D Reidel Publishing Company, Dordrecht - Holland.)

7

The surface channel, which could be used to communicate between ship and SSN at ranges to 185 km (100 nmi), typically has less time dispersion than the long range sofar channel. Multipath spreads in the surface channel may be a few hundred ms. The time variance, however, may be much greater than in the sofar channel. The primary cause of fluctuation of the received sound is the moving sea surface (ref 4,6,7), which creates multipath interference by reflection and scattering. The faster fluctuations are caused by sea-surface motion, and as can be seen in figure 6, the spectrum of the fluctuation duplicates the spectrum of the waves (ref 6).

The acoustic wave is scattered largely by reflection from the ocean surface or bottom, although scattering can also occur in returns from particles, fish, and organisms in the water. The scatter in a sonar pulse returning to the sonar receiver is called reverberation. Figure 7, from reference 8, shows representative reverberation levels versus time for three different locations in the Atlantic Ocean. The top trace was from a site on the European continental rise, the middle trace from a site north of the Azores plateau, and the bottom trace from a mid-Atlantic site. Scatter returns have sharp rises and slow falls that drop off as $-10(n) \log(t)$, where the value of n depends upon the scattering process. For example, n = 2 corresponds to an infinite uniform distribution of isotropic scatters. More common is n = 3, which results from a boundary layer of isotropic scatters that can occur at the surface, at the bottom, and from layers of marine organisms.
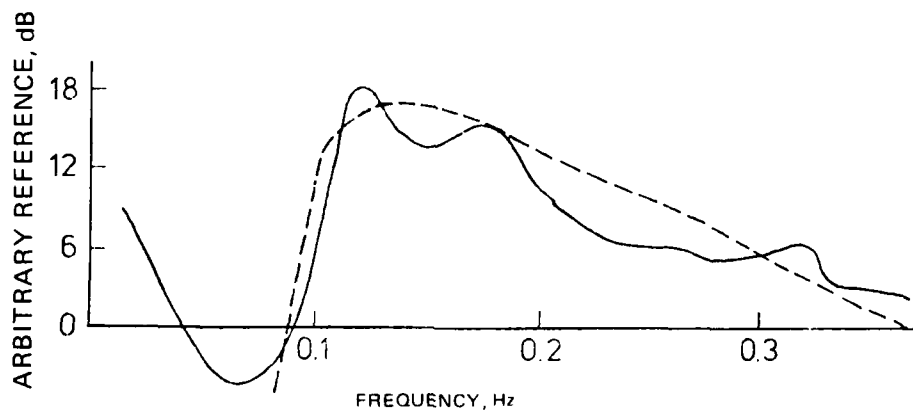

Figure 6. Modulation spectrum of the envelope of a signal received from a 275-Hz cw source towed at 2.7 knots at a range of 23 miles. Dashed line is a Neuman-Pierson wave spectrum for a wind speed of 20 knots. Analysis bandwidth is 0.02 Hz. (From ref 6. Reprinted by permission of D Reidel Publishing Company, Dordrecht - Holland.)

7. RL Veenkant, Investigation of the Propagation Stability of a Doubly Spread Underwater Acoustic Channel, IEEE Transactions on Acoustics, Speech and Signal Processing, vol ASSP-25, no. 2, April 1977.

8. RD Chapman, Sound Scattering in the Ocean, p 161 of Underwater Acoustics, vol 2, edited by VM Albers, Plenum Press, New York, 1967.
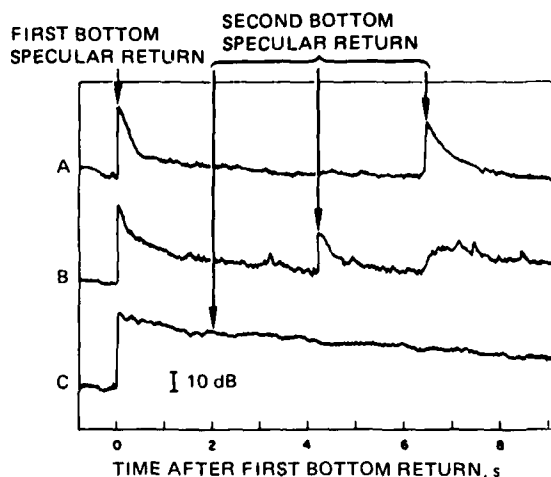
FIRST BOTTOM
SPECULAR RETURN

SECOND BOTTOM
SPECULAR RETURN

A

B

C

$\underline{\text{I}}$ 10 dB

| | | | | |
| 0 | 2 | 4 | 6 | 8 |

TIME AFTER FIRST BOTTOM RETURN, s

Figure 7. Representative bottom reverberation level
versus time traces obtained in the 0.8–1.6 kHz band
at three Atlantic Ocean sites. A — on the European
continental rise, B — north of the Azores plateau,
C — mid-Atlantic. (From ref 8. Reprinted by
permission.)

CHANNEL MODEL

Good channel models are essential for the design and evaluation of communication
systems. The many types of models can generally be grouped into two categories: macro-
scopic and microscopic (ref 9). These terms, although not universal, help delineate the dif-
ferences between the models.

Macroscopic models characterize the signal propagation and typically provide infor-
mation concerning signal ray paths and path losses. They are useful for estimating com-
munication range, depth, and coverage. Since several good macroscopic propagation models
are available, this category is discussed no further.

Microscopic models, on the other hand, describe what happens to the shape of the
signal as it propagates from transmitter to receiver. These models, frequently described in
terms of stochastic time-variant filters, are useful in designing and/or evaluating signaling
schemes for communications. Our knowledge of the microscopic channel directly affects
the efficiency to which we can design a signal processing scheme. The more we know, the
better.

Figure 8 is a major component block diagram of a digital communication system
that sends digital information via two states, referred to as "mark" and "space." Corre-
spondingly, there are two pulse waveforms, and the transmitter sends one of the two pulse
waveforms for each binary digit. The transmitted pulse waveforms are defined as $s_I(t)$,

9. J Johnsen, Models of the Underwater Acoustic Channel, Eighth International Congress on Acoustics,
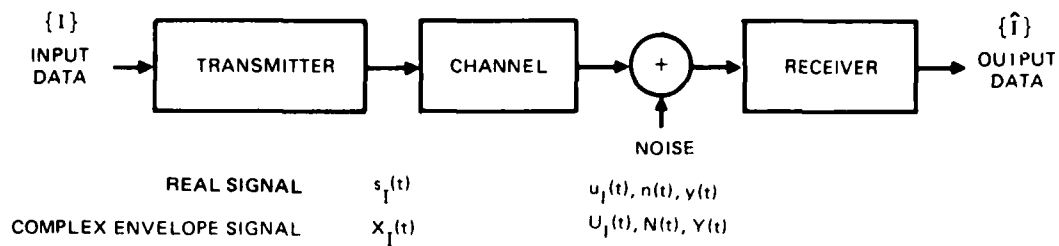London 1974.

Figure 8. Communication system model.

where I is either an M or an S, for mark or space. The response of the channel to $s_I(t)$ is $u_I(t)$. Noise, $n(t)$, is added to $u_I(t)$ at the receiver to create the observed waveform, $y(t)$.

Complex mathematical representation of signals, filters, and noise is used in this report. For example, if the actual transmitted waveform is represented by the expression

$$s_I(t) = g_I(t) \cos [wt + \phi(t)],\tag{1}$$

it can also be written as

$$s_I(t) = R\ell\, g_I(t)\, e^{i\phi_I(t)}\, e^{iwt}.\tag{2}$$

where $R\ell$ means "take the real part of what follows."

By defining the complex envelope as

$$X_I(t) = g_I(t)\, e^{i\phi_I(t)}.\tag{3}$$

we can relate the actual waveform (at frequency w) to the complex envelope (at base band) as

$$s_I(t) = R\ell\, X_I(t)\, e^{iwt}.\tag{4}$$

Similar relationships (ref 10, chapter 1) hold for the $u_I(t)$, $n(t)$, and $y(t)$ shown in figure 8. The complex envelope of the channel response $u_I(t)$ is $U_I(t)$, of the additive noise $n(t)$ is $N(t)$, and of the received signal $y(t)$ is $Y(t)$.

NOTE

For the remainder of this section we will be describing the channel model, which is independent of which signal - mark or space - is sent. Therefore, the subscript I from $s_I(t)$, $u_I(t)$, $X_I(t)$, and $U_I(t)$ is omitted. In section 3, the subscripts are used.

---

10. C Helstrom, Statistical Theory of Signal Detection, Pergamon, Second Edition, Oxford, 1968.

10

If the channel were time invariant, we could model it as a linear filter that would be completely defined by its complex impulse response $h(\tau)$, which is the response of the filter to an input impulse that occurred τ seconds ago. The frequency response, $H(f)$, of this filter is defined as the Fourier transform of $h(\tau)$, where the transform is taken over the delay variable

$$H(f) = \int_{-\infty}^{\infty} h(\tau) e^{-i2\pi f\tau} d\tau \ . \tag{5}$$

The underwater acoustic channel, however, is time variant. Changes occur to the channel transfer function within time periods of a message, and in some cases within a few transmitted bits. Therefore, we must show this time dependence explicitly by using a time-variant filter specified by the impulse response $h(\tau, t)$, which is the response of the filter at time t due to an input at time $t-\tau$. The time-varying frequency response, $H(f, t)$, is the Fourier transform of $h(\tau, t)$, where the transform is taken as the variable τ. $H(f, t)$ is the response of the filter at time t to an input sine wave of frequency f. Note that the response to a specular sine wave at frequency f_0 is in general nonspecular and contains energy in the frequency band about f_0.

The channel output signal, which is the convolution of the input signal with the channel response, is given by the relationship

$$U(t) = \int_{-\infty}^{\infty} h(\tau, t) X(t-\tau) d\tau \ . \tag{6}$$

The channel response can also be written in terms of the frequency response $H(f, t)$ and signal spectrum $\widetilde{X}(f)$ as

$$U(t) = \int_{-\infty}^{\infty} H(f, t) \widetilde{X}(f) e^{i2\pi ft} df \ . \tag{7}$$

$H(f, t)$ is a random process that must be described by its statistics. One very useful statistic is the channel two-frequency correlation function, defined as follows:

$$R(\Delta f, \Delta t) = E[H(f, t) H^*(f + \Delta f, t + \Delta t)] \ , \tag{8}$$

where E is the expected value (or average) of the product over all possible realizations in the ensemble of $H(f,t)$ and $H(f + \Delta f, t + \Delta t)$. The asterisk means "take the complex conjugate of."

Another useful statistic is the double Fourier transform of the two-frequency correlation function of Δf and Δt. Define the scattering function as $\sigma(\tau, \nu)$ where

$$\sigma(\tau, \nu) = \int_{-\infty}^{\infty} \int_{-\infty}^{\infty} R(\Delta f, \Delta t) e^{i2\pi(\tau\Delta f - \nu\Delta t)} d\Delta t \ d\Delta f \ . \tag{9}$$

We can interpret the scattering function as the ratio of channel output power per unit time per unit frequency to input power. Figure 9 is a sketch of what a scattering function might look like. Two propagation paths have been shown that are separated in frequency and time. Each path is spread in frequency and time, meaning that each path fades and has time distortion. The total overall frequency spread, B, and time spread, T_L, are limitations to the adaptive signal processing schemes. The minimum time that we can observe the output of the channel for the purpose of making a channel response estimate is T_L seconds. However, the channel response changes in a time period of about 1/B seconds. If we are to use the channel response estimate in an adaptive signal processing scheme, 1/B must be much greater than T_L. Thus, for adaptive signal processing we want

$$BT_L \ll 1 \ ,$$

and this condition is called underspread. Channels wherein BT_L is greater than one are called overspread. Because the underwater acoustic channels can have BT_L products approaching unity (ref 7), we would like to compare tonal FSK to RAKE under such conditions to determine which would be the best approach.

Figure 10 depicts a surface channel between a ship and a submarine. The ray traces of the sound propagation are intended not to be precise but to provide a simple example that can be visualized. Between ship and submarine there exist multiple paths, and in figure 10 we have tried to show two of them. Each path consists of a number of subpaths due to scattering from the surface and from particles in the ocean. Each path or group of subpaths has a path loss, a_k, and some mean path delay, τ_k. In the system shown, the moving elements are the ship, the submarine, and (in response to wind and current) the medium (ocean) itself. Thus, each path has a velocity v_k.
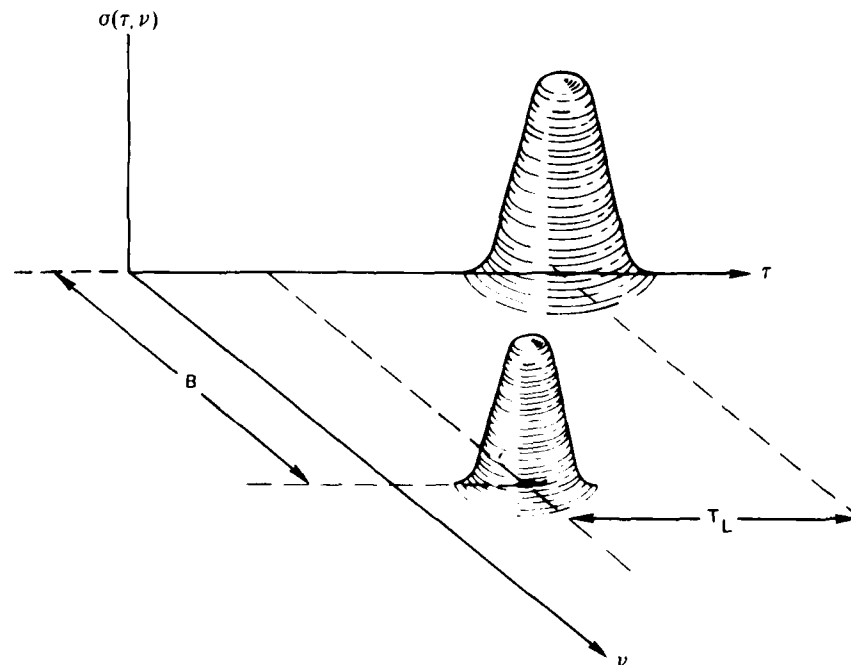

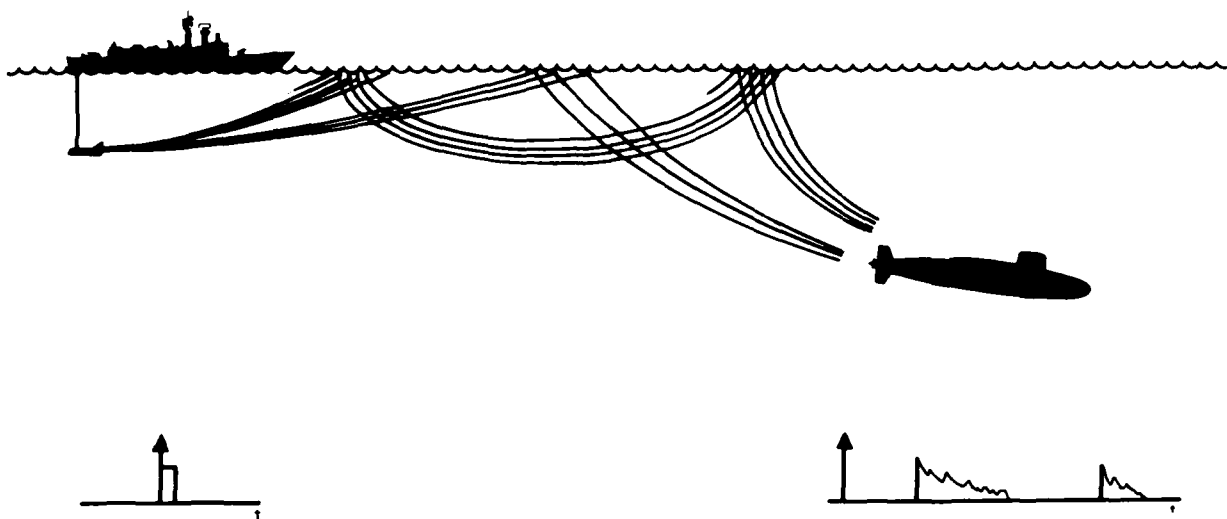Figure 9. Channel scattering function for a two-path channel.

12

Figure 10. Surface channel between ship and submarine.

First, let us consider an arbitrary subpath with mean sound velocity c. Let the mean velocity between the platforms be v, with the platforms initially located d_o apart. Figure 11 *is a graph of the distance traveled by the sound waveform and the receive platform, where* both are referenced to the transmit platform. Consider a point on the transmit waveform s(t) that occurs at time t′. The output of the channel is u(t), which is a replica of s(t′) but occurs much later than t′ because of the propagation delay. From figure 11 we have u(t) = s(t′) when

$$(t - t') c = d_o + vt \tag{10}$$

or

$$t' = t\left(1 - \frac{v}{c}\right) - \frac{d_o}{c} \quad . \tag{11}$$

We can substitute this value of t′ into s(t′) to get

$$u(t) = s\left[t\left(1 - \frac{v}{c}\right) - \frac{d_o}{c}\right] \tag{12}$$

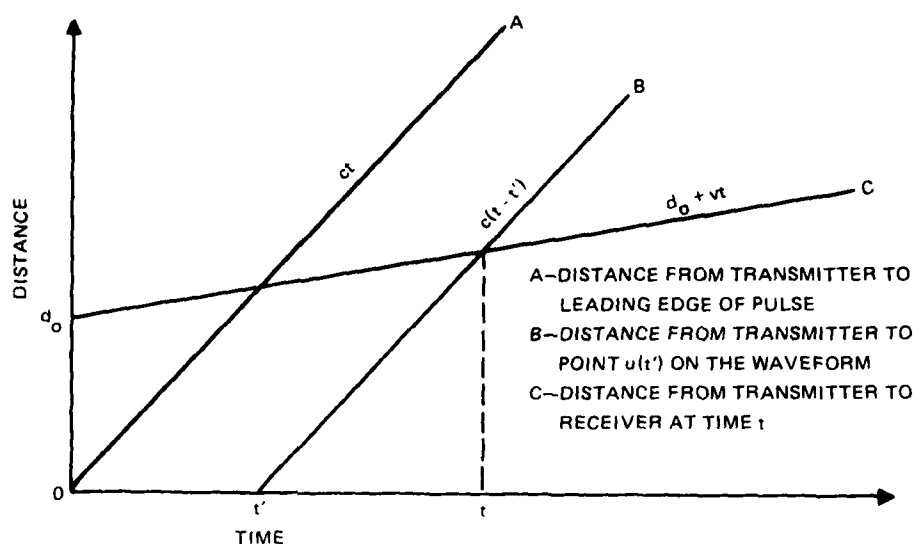$$u(t) = s\left(t - \beta t - \tau_o\right) , \tag{13}$$

13

Figure 11. Propagation distances of sound pulses.

where we have defined

$$\beta = v/c \qquad (14)$$

and

$$\tau_0 = \frac{d_0}{c} . \qquad (15)$$

The output of the channel is the sum of delays and scattered replicas of the transmitted pulse (ref 11, p 352-367). Let $u_j(t - \tau_j)$ be the scattered output pulse that occurs at time τ_j. Then the channel output waveform can be written as

$$u(t) = \sum_{j=1}^{L} u_j(t - \tau_j) . \qquad (16)$$

where we assume that L such pulses may overlap. A single scattered pulse may be written as the sum of a number of subpaths, where the channel intensity for each subpath may be similar to the shape of the scatter pulses in figure 7. The reflection from each subpath randomly

---

11. M Schwartz, WR Bennett, and S Stein, Communication Systems and Techniques, McGraw-Hill Book Company, New York, 1966.

14

affects the amplitude and phase of the pulse. Let a_{jk} be the amplitude of the kth subpath in the jth scattered pulse. Then we can express the scattered pulse as

$$u_j(t - \tau_j) = \sum_{k=1}^{n} a_{jk} \, s\left(t - \tau_j - \tau_{jk} - \beta_{jk}t\right) .$$
(17)

Substituting the Fourier transform definition of s(t) and rearranging terms gives

$$u_j(t) = \int_{-\infty}^{\infty} e^{i2\pi ft} \, S(f) \left[\sum_{k=1}^{n} a_{jk} \, e^{-i2\pi f(\tau_{jk}+\beta_{jk}t)} \right] df .$$
(18)

The expression enclosed in brackets is the time-variant transfer function for the channel. This transfer function is a wideband representation, given by the expression

$$\widetilde{H}_j(f, t) = \sum_{k=1}^{n} a_{jk} \, e^{-i2\pi f(\tau_{jk}+\beta_{jk}t)} .$$
(19)

If we instead substitute for s(t) its complex envelope definition, then substitute for X(t) its Fourier transform, we get the complex-envelope narrowband transfer function given by the expression

$$H_j(f, t) = \sum_{k=1}^{n} a_{jk} \, e^{-i2\pi(f+f_0)(\tau_{jk}+\beta_{jk}t)} ,$$
(20)

where f_0 is the center frequency for a narrowband channel. $\widetilde{H}_j(f, t)$ should be used for wideband channels and $H_j(f, t)$ may be used for narrowband channels. Taking the Fourier transforms of (19) and (20) gives the channel impulse response for the wideband channel

$$\widetilde{h}_j(\tau, t) = \sum_{k=1}^{n} a_{jk} \, \delta\left(\tau - \tau_{jk} - \beta_{jk}t\right) ,$$
(21)

and for narrowband channels

$$h_j(\tau, t) = \sum_{k=1}^{n} a_{jk} \, e^{-i2\pi f_0(\tau_{jk}+\beta_{jk}t)} \, \delta\left(\tau - \tau_{jk} - \beta_{jk}t\right) .$$
(22)

The complex envelope of the jth received pulse is as follows:

$$U_j(t) = \sum_{k=1}^{n} a_{jk} \, X\left(t - \tau_{jk} - \beta_{jk}t\right) e^{-i2\pi f_0(\tau_{jk}+\beta_{jk}t)} .$$
(23)

To find the two-frequency correlation functions, we need to know something about the statistical dependency of the subpaths. It is a temptation to assume that they are independent since they are scattered from independent particles or organisms in the ocean or they represent reflected energy from different patches of the ocean surface. Although we yield to this temptation, the statistical dependency of the subpaths is an issue for further research.

The Doppler shift factors β_{jk} are assumed to be Gaussian independent random variables that are identically distributed within a scatter pulse. The variance and mean for the jth scatter pulse are taken as σ_j and m_j. Computing the expected value according to equation (8) gives

$$R_j(f, t, f + \Delta f, t + \Delta t) = \sum_{k=1}^{n} \overline{|a_{jk}|^2} \; e^{-i2\pi\Delta f \tau_{jk}} \; \exp\left(-2\pi^2\sigma_j^2\theta^2 - i2\pi m_j\theta\right) , \qquad (24)$$

where

$$\theta = (f + f_0)t - (f + f_0 + \Delta f)(t + \Delta t) . \qquad (25)$$

The two-frequency correlation function is, in general, nonstationary in frequency and in time. As Δf or Δt gets large, the correlation exponentially goes to zero.

For narrowband channels, f and Δf are confined to a frequency region near zero, so that f and $f+\Delta f$ are much smaller than f_0. In this case, the correlation function becomes stationary:

$$R_j(\Delta f, \Delta t) = \sum_{k=1}^{n} \overline{|a_{jk}|^2} \; e^{-i2\pi\Delta f \tau_{jk}} \; \exp\left(-2\pi^2 B_j^2\Delta t^2 - i2\pi\nu_j\Delta t\right) . \qquad (26)$$

where we have defined the fade rate as follows:

$$B_j = \sigma_j f_0 . \qquad (27)$$

and the mean Doppler shift as follows:

$$\nu_j = m_j f_0 . \qquad (28)$$

This narrowband approximation results in a channel model with the same properties as an hf channel model (ref 12), where the channel correlation function is a function of only the frequency separation (Δf) and time separation (Δt). This approximation is applicable to signaling schemes in which the bandwidth is much less than the center frequency and the transmit and receive platform velocities are very small.

In wideband acoustic systems which use bandwidths that are a significant fraction of the center frequency, the above correlations do not apply and the correlation must be

12. CC Watterson, J Juroshek and W Bensema, Experimental Confirmation of an HF Channel Model, IEEE Transactions on Communication Technology, vol 18, no 6, p 792-803, December 1970.

recomputed by using the wideband model. The resulting expression has the same form as equation (24); in this case, however,

$$\theta = ft - (f + \Delta f)(t + \Delta t) .$$ (29)

The fade rate depends upon the frequency and time of observation. If we observe our received spectrum at frequencies f and f + Δf at the same time, t, the relative fade rate of the two spectral amplitudes is given by $\sigma_j \Delta f$. Intuitively, we want this rate to be small to allow as wide a correlation bandwidth as possible. Fixed matched-filter systems would like it to be zero. Similarly, if we examine the same frequency of the received spectrum at times t and t + Δt, the rate of change (fade rate) is given by $\sigma_j \Delta t$. Again we want this rate to be small to give adaptive receivers a chance to "learn" the channel output. Ideally, therefore, we want σ_j to be small.

An important statistic that is easily measured is the "multipath intensity profile" (ref 11, page 361), $r(\tau)$, which is the Fourier transform of the two-frequency correlation function on Δf, with the time variable (Δt) set equal to zero. Mathematically, for narrowband channels

$$r_j(\tau) = \int_{-\infty}^{\infty} R_j(\Delta f, 0) \, e^{i2\pi(\Delta f)\tau} \, d(\Delta f) .$$ (30)

For the correlation function given in (26), we have

$$r_j(\tau) = \sum_{k=1}^{n} \overline{|a_{jk}|^2} \, \delta(\tau - \tau_{jk}) .$$ (31)

Examples of this statistic are shown as figure 7. Rectifying the received sonar return and averaging from scan to scan (possibly by using a memory oscilloscope) gives an estimate of the multipath intensity profile. The values of $|a_{jk}|^2$ have a sharp rise and then fall off as $- 10p \log t$, where p is a factor near 3.

Figure 12 is a block diagram of the narrowband channel model. The number of paths in the model depends upon the situation, and in some cases there may be only one path that is entirely scatter. The average gains (g_j) have been shown separately, to emphasize the differences of the paths. The path scatter response, $h_j(\tau, t)$, is Gaussian zero mean scatters with fade rates (bandwidths) of $2B_j$ hertz and Doppler shift ν_j.

Because the output of the scatter for the narrowband model consists of delayed replicas of the transmitted signal, an obvious model for each path of the channel consists of a tapped delay line. The taps are located at time delays $\tau_{jk}(k = 1, 2, ... n - 1, n)$ equal to the path time delays, where n is the number of subpaths. On each tap there is a complex multiplier α_{jk}, called a tap gain, that attenuates the amplitude and shifts the phase of the
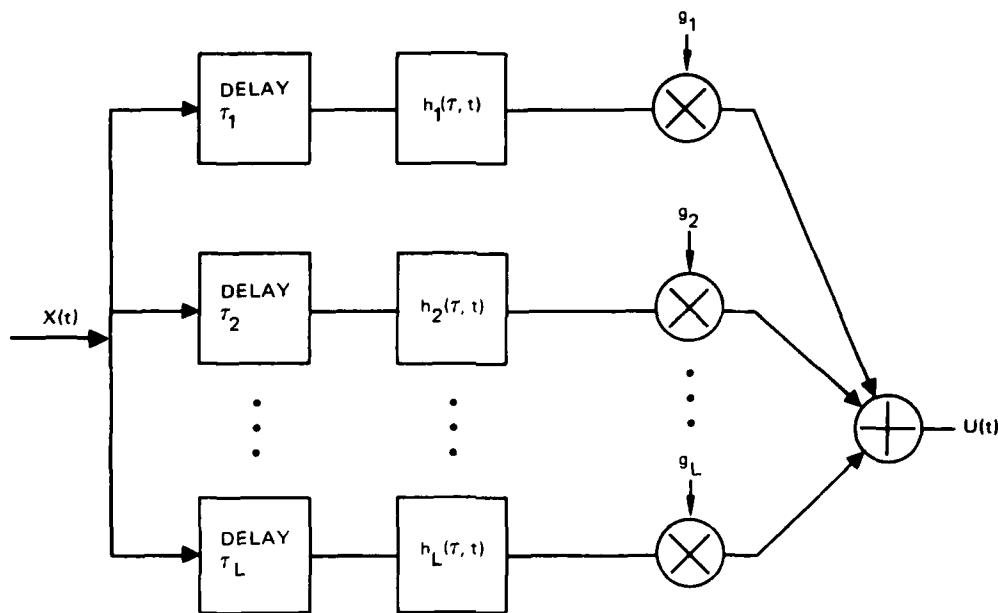
17

Figure 12. Block diagram of a narrowband underwater acoustic
channel model.

tap output to correspond to the received subpath signal. The tap multiplier is defined as

$$\alpha_{jk} = a_{jk} \, e^{-i2\pi f_o(\tau_{jk}+\beta_{jk}t)} .$$

Figure 13 is a block diagram of the tapped delay line model for the channel. The received
subpath signals randomly fade with time, causing the tap gains to be random processes. The
model is specified when we give the tap delays and the statistics of the tap gains. Figure 14
is a sketch of the power spectrum for one of the tap-gain functions. Only two parameters
are needed to specify the power spectrum: the mean (ν_j) and the variance (B_j^2). The mean
is called the Doppler shift, and twice the standard deviation is called the frequency spread.

In this section, two mathematical models—a wideband and a narrowband model—have
been derived for the underwater acoustic channel. The wideband channel model (a general
channel model) permits signals with large bandwidths and channels with large Doppler shifts.
But since the statistics for this model are nonstationary, the application of this model to
communications analysis is extremely difficult.

A model with stationary statistics is derived from the general model by assuming that
the signals are narrowband (ie, the signal bandwidth is less than the transmitted center
frequency) and that the velocities of the transmit and receive platforms are very small. The

18

narrowband model is analogous to models used for hf. Thus there exists a subset of acoustic channels that can be modeled like hf channels. The next section takes advantage of this fact to apply existing mathematical analysis from hf channels to that subset of underwater acoustic channels.
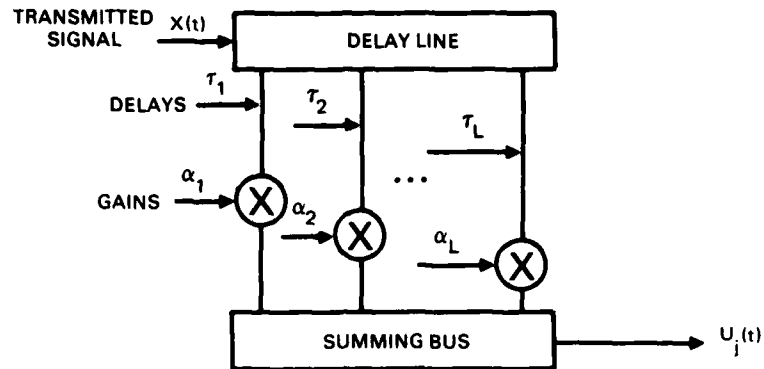

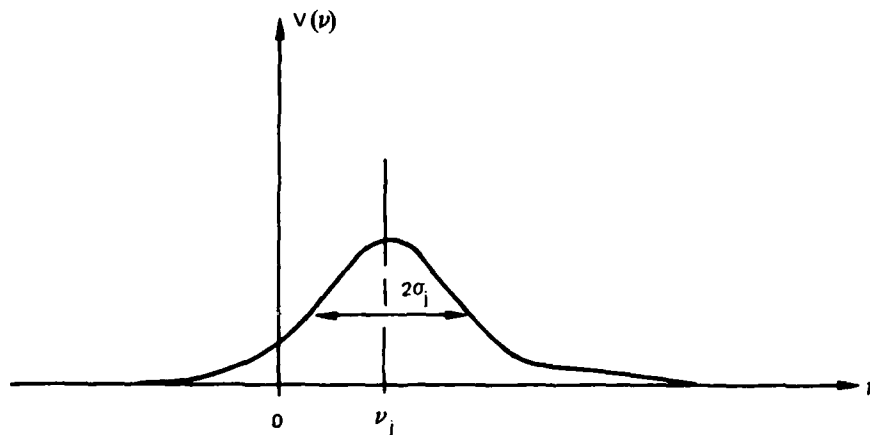Figure 13. Tapped delay line model for a propagation path with scatter.

Figure 14. Tap-gain power spectra.

3. COMMUNICATION SIGNALING

The underwater acoustic channel can provide important communication links for Navy command and control. The acoustic channel, however, is degraded by severe multipath dispersion, Doppler shifts, and fading, which seriously distort the transmitted signal. These channel distortions can cause excessively high error rates unless sophisticated signaling schemes are used. In this section, two schemes are discussed: a tonal system with diversity and a direct sequence spread spectrum system. Both systems use frequency shift key (FSK) modulation and bit decision periods longer than the channel multipath time spread. FSK modulation is selected because it provides a lower bit error rate than phase shift key modulation for high channel fade rates (ref 13). Until this report, no definitive comparison of these two modulation schemes has been made for acoustic channels, where the rate of change of the channel response approaches the reciprocal of the time delay spread. We give results on the probability of error analysis and compare the systems.

We confine our analysis to the subset of acoustic channels that can be modeled as being narrowband and having small Doppler shifts. This does not restrict the time variability (B) or the extent of multipath time spread (T_L) present in the channel. The restriction here is to signals with bandwidths less than the transmitted center frequency and to transmit and receive platforms with small velocities. It was shown in the last section that this subset of channels can be mathematically modeled similarly to hf channels, allowing us to apply existing communication performance analysis to the underwater acoustic channel.

TONAL FSK WITH DIVERSITY

Figure 15 shows the basic concept behind the use of long cw pulses for signaling on multipath channels. The pulse lengths are made much longer than the channel multipath time delay spread. They are modulated with digital information by keying either the pulse phase (PSK) or center frequency (FSK). For channels with severe time dispersion, the channel pulse rate is quite low. Data rate can be increased by using multiple phases (MPSK) or multiple frequencies (MFSK). For this analysis we concentrate on binary FSK signaling. On fading channels, bit detection errors occur primarily when the received signal fades, causing a momentary low signal-to-noise ratio. A common technique to minimize the duration of signal fade is to process several independent channels containing the same transmit signals. If the channels fade independently, it is unlikely that all the channels fade at the same time. This technique is called "diversity." Diversity channels can be designed into the system by transmitting more than one message in frequency or time or by using widely spaced antenna systems. Hahn (ref 14) has shown that most of the diversity improvement occurs when the number of diversity branches, L, is 2 and that very little additional gain occurs for values of L greater than 4. We use L = 2 and L = 4 to illustrate the performance of tonal modulation schemes. The received pulse illustrated in figure 15 consists of the sum of the multiple paths and can be described in terms of its transient and steady state portions. The beginning and end of the received pulse are transient since the individual multipath signals arrive during the

13. PA Bello and BD Nelin, The Influence of Fading Spectrum on the Binary Error Probabilities of Incoherent and Differentially Coherent Matched Filter Receiver, IRE Transactions on Communication Systems, p 160-168, June 1962.

14. PM Hahn, Theoretical Diversity Improvement in Multiple Frequency Shift Keying, IRE Transactions on Communication Systems, p 117-184, June 1962.
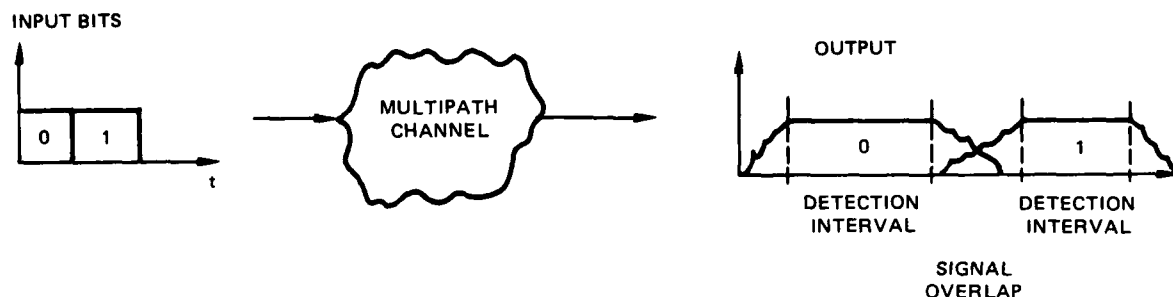
Figure 15. Concept for long duration bits. Bit length must be long compared to multipath spread. Data rate per channel is low. (High data rates are achieved by using parallel tones.) Receiver processes detection intervals.

multipath spread. Once all the paths have arrived, the sum of the paths becomes a steady state value that depends upon the amplitude and phase of the individual paths. These characteristics can be modeled as a Gaussian process, where the amplitude is Rayleigh and the phase is uniformly distributed. It is primarily the steady state portion that is used by the receiver to demodulate the information because this part of the signal pulse envelope is known at the receiver (with the exception of mark or space center frequency) and is free of intersymbol interference. Some receivers (eg AN/FGC-29, AN/UCC-1) ignore the transient part of the signal and process the entire pulse as if it were steady state, whereas other receivers (eg Kineplex, Link-11, and Kathryn— AN/GSC-10) use only the time slice of the receive signal that is steady state.

The concept hinges upon underspreading of the channel. If B is the frequency spread and T_L is the time spread of the channel, we assume that the tonal pulse duration T is much less than the time required for the channel to change, or

$$T < 1/B .\tag{32}$$

Since the bandwidth (W) of the FSK signal must be less than the reciprocal of the time dispersion to avoid selective fading, we have

$$W < 1/T_L .\tag{33}$$

For constant wave pulses, TW is approximately equal to unity. This implies that $BT_L < 1$, which is the condition for underspread.

In a tonal FSK system designed for the underwater acoustic channel, the channel can deviate from the basic design assumptions and approach an overspread condition in two ways. First, the time spread (T_L) of the multipath may be considerably longer than was assumed, so that the product BT_L is increased. The steady state portion is diminished or possibly eliminated, and the received waveform cannot be approximated by its steady state portion. This situation might correspond to using the communication system over longer ranges than had been anticipated. Second, the multipath spread may be small but the time rate of change of the multipath B may be too great, and BT_L again approaches unity. This situation might correspond to a cold water channel, where the surface waves cause fast fading of the signal. Although the steady state portion is not corrupted by the late arrival of multipath, the amplitude and phase of the received signal do change during the steady state portion. The bandwidth of the received signal is increased, causing interference between the mark and space information.

Ideally, we would like to know the probability of error for arbitrary fade rate (B) and time dispersion (T_L) as the product BT_L approaches unity. Although we don't have this analysis, Bello and Nelin (ref 1,13) have made separate studies of (1) slow fade rates but severe time dispersion and (2) minor time dispersion but severe fade rates. The matched filter receiver was analyzed for incoherent FSK and coherent PSK for arbitrary orders of diversity, and the probabilities of error were derived. We briefly summarize this work for incoherent FSK.

Figure 16 depicts a simple model of an incoherent matched filter receiver for one branch of a diversity receiver. The complex envelopes of the mark and space waveforms are given by the following relationships:

$$X_M(t) = \begin{cases} \sqrt{\dfrac{2E}{T}} \; e^{-i\pi t/T} & (0 \leqslant t \leqslant T) \\ \\ 0 & (\text{for t otherwise}) \end{cases} \tag{34}$$

and

$$X_S(t) = \begin{cases} \sqrt{\dfrac{2E}{T}} \; e^{i\pi t/T} & (0 \leqslant t \leqslant T) \\ \\ 0. & (\text{for t otherwise}) \end{cases} \tag{35}$$

The outputs from the matched filters are given by the equations

$$U = \int_0^T y(t) \, X_M^*(t) \, dt \tag{36}$$

and

$$V = \int_0^T y(t) \, X_S^*(t) \, dt \, , \tag{37}$$

where y(t) is the received-signal complex envelope and T is the band duration. If there are K diversity channels and a zero-threshold decision device, a mark is chosen as the transmitted signal when

$$q = \sum_{j=1}^{k} |U_j|^2 - |V_j|^2 > 0 \, . \tag{38}$$
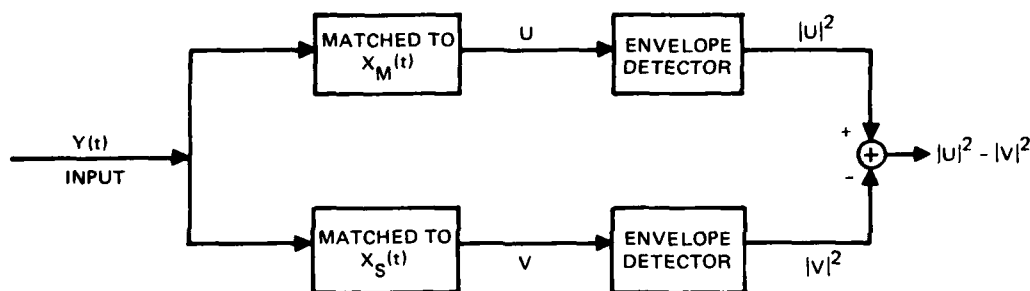
and a space is chosen when $q < 0$.

Figure 16. Model of incoherent matched filter receiver.

There are two ways the receiver can make an error. It can decide that a mark is present when in fact a space was sent, and, similarly, it can decide a space is present when in fact a mark was sent. Daly (ref 15) solved these equations for the narrowband Gaussian channel model and calculated the probability of error for several channel models.

The error probabilities depend upon four factors:

1. Number of diversity channels (K)

2. Number of propagation paths

3. The path description (R_k, T_k, D_k) for each propagation path, where

$$R_k = \frac{\text{Received signal power of kth path}}{\text{Total received signal power of all paths}}$$

$$T_k = \frac{\text{Time delay of kth path}}{\text{Band duration}}$$

$$D_k = (\text{Doppler shift of kth path}) \times (\text{band duration})$$

4. Signal-to-noise ratio of a single diversity channel at the receiver input, where

$$SNR = \frac{\text{Signal power in a single diversity channel}}{\text{Noise power in a single diversity channel}}$$

Tables 1 and 2 summarize the channels analyzed by Daly, and figures 17 and 18 present the respective probability of error results, assuming dual diversity.

15. RF Daly, Analysis of Multipath Effects on FSK Error Probability for a Simple HF Channel Model, Stanford Research Institute Memorandum 1, Project 4554 Control SD-189, Office of Secretary of Defense, Washington, DC, February 1964.

Case	Number of Paths	T_1	T_2	D_1	D_2	R_1	R_2
1	1	0	0	0	0	1.0	0
2	2	0	0	0.05	-0.05	0.5	0.5
3	2	0.025	-0.025	0	0	0.5	0.5
4	2	0.025	-0.025	0.05	-0.05	0.5	0.5
5	2	0	0	0.1	-0.1	0.5	0.5
6	2	0.05	-0.05	0	0	0.5	0.5
7	2	0.05	-0.05	0.05	-0.05	0.5	0.5
8	2	0.05	-0.05	0.10	-0.10	0.5	0.5
9	2	0.10	-0.10	0	0	0.5	0.5
10	2	0.20	-0.20	0	0	0.5	0.5

Table 1. Key to figure 17. (From ref 15.)

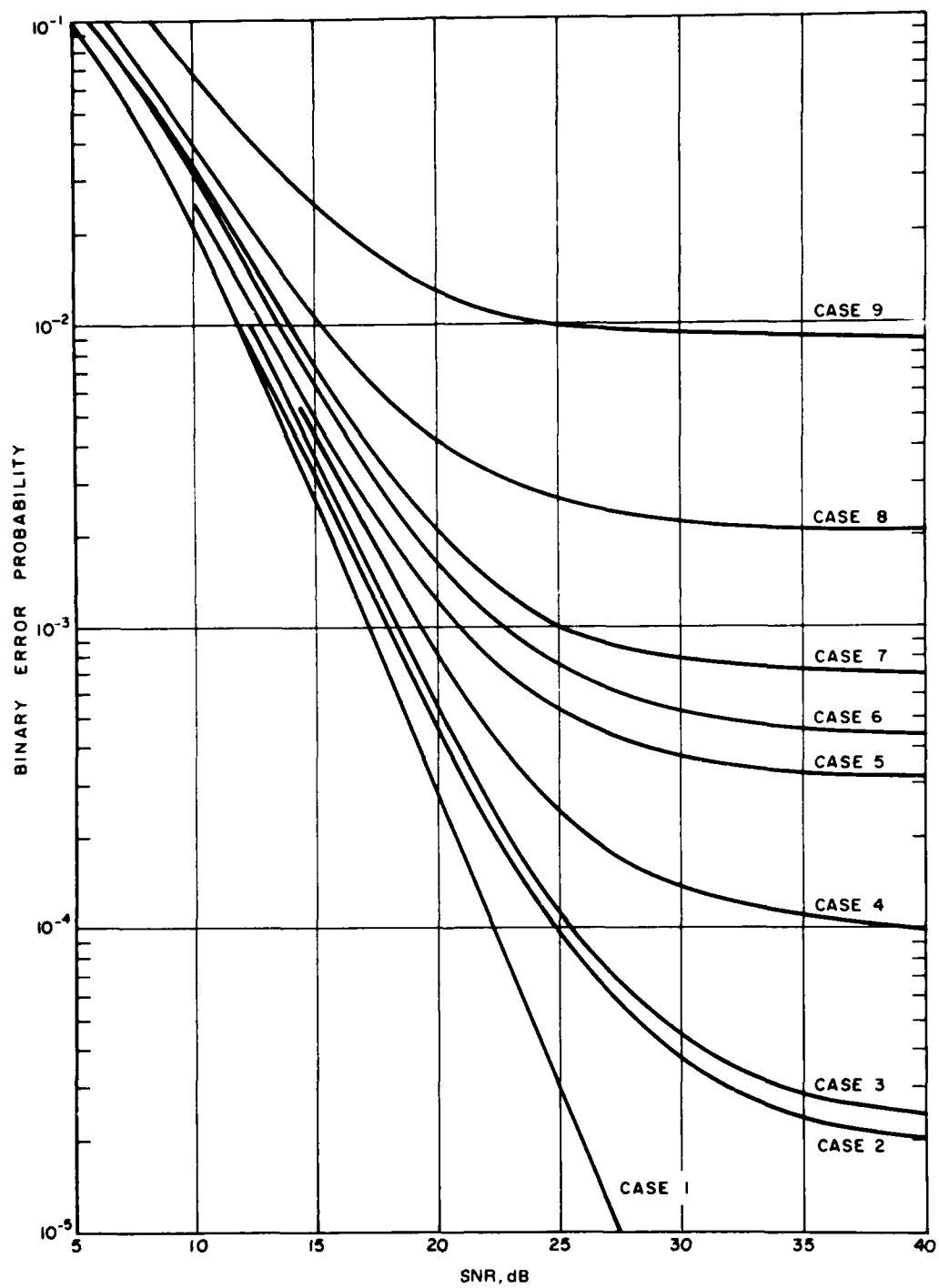| Case	Number of Paths	T_1	T_2	T_3	T_4	T_5	D_1	D_2	D_3	D_4	D_5	R_1	R_2	R_3	R_4	R_5
1	1	0					0					1				
11	3	0	0	0			-0.025	0	0.025			0.25	0.5	0.25		
12	2	0	0				0.05	-0.05				0.667	0.333			
13	2	0	0				0	-0.20				0.8	0.2			
14	5	-0.05	-0.025	0	0.025	0.05	0.1	0.05	0	-0.05	-0.1	0.125	0.125	0.5	0.125	0.125
15	5	-0.1	-0.05	0	0.05	0.1	0.05	0.025	0	-0.025	-0.05	0.125	0.125	0.5	0.125	0.125
16	3	-0.1	0	0.1			0	0	0			0.25	0.5	0.25		
17	2	0.05	-0.1				0	0				0.667	0.333			
18	2	0.05	-0.1				0.05	-0.05				0.667	0.333			
19	2	0.1	-0.4				0	0				0.8	0.2			

Table 2. Key to figure 18. (From ref 15.)

Figure 17. Phase-discontinuous FSK error probability, dual diversity, cases 1-9. (From ref 15.)
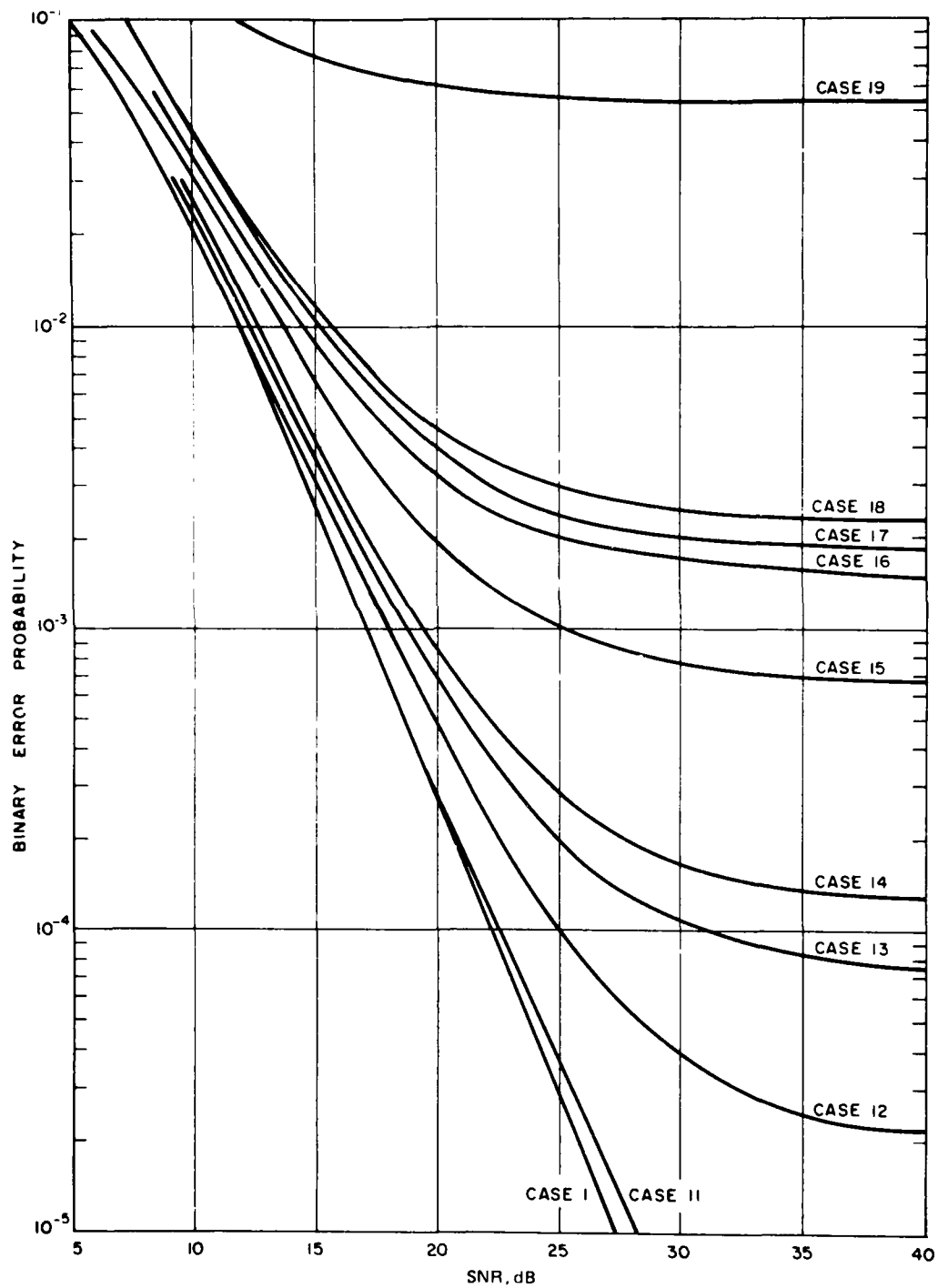
25

Figure 18. Phase-discontinuous FSK error probability, dual diversity, cases 11-19. (From ref 15.)

26

The most significant property of these curves is the existence of an irreducible error probability when the channel introduces time delays and Doppler shifts. A system using such a channel will make errors even when the signal-to-noise ratio is infinite.

For channels with severe time dispersion (ref 1,13), the irreducible bound increases as the channel multipath spread approaches the pulse width, T. Figure 19 shows the irreducible error probability as a function of the relative data rate given by the expression

$$d = \frac{1}{B_c T} ,$$
<div align="right">(39)</div>

where B_c is the correlation bandwidth. Since B_c is inversely proportional to the multipath time spread, the relative data rate(d) is proportional to the ratio

$$\frac{\text{channel multipath time spread}}{\text{pulse width duration}} .$$

Two curves are shown in figure 19 — one for dual diversity, one for quad diversity. The basic assumption is that the channel response does not change significantly in T seconds; therefore, the channel fade rate (B) is less than 1/T. Even with this restriction, the tonal scheme cannot tolerate large channel multipath time spread compared to the pulse width (T).

Figure 20 shows the irreducible error probability for channels with severe frequency spread (fast fading). The irreducible error probability increases as the fade bandwidth (B) approaches the reciprocal of the pulse duration (T). The basic assumption is that the multipath time spread (T_L) is much less than the pulse width (T). We could interpret T as the duration of the steady state portion of the received pulse and E as the energy of that portion. The multipath transients, then, would be outside the period T. Even though the fade-rate time-spread factor (BT_L) is quite large, figure 20 would still be meaningful. The irreducible error rate is caused by amplitude and phase changes during the steady state portion (T) and by intersymbol interference between the mark and space symbols, assumed to be separated in frequency by 1/T Hz.

We can conclude from figures 19 and 20 that the probability of error of tonal FSK signaling with diversity is sensitive to changes in channel fade rate and time dispersion. When either the channel time spread (T_L) or the fade period (1/B) approaches the pulse width (T), the irreducible error probability increases toward 1/2.

RAKE AND PROBE SIGNALING

Although tonal modulation schemes have been the traditional approach to signaling on time-dispersed multipath channels, there has been interest in using broadband waveforms to gain some protection from enemy detection. The class of waveforms of interest uses direct sequence spread spectrum modulation to achieve wide bandwidths (much wider than the reciprocal of the pulse width, T) and uniformly low signal energy per hertz. The demodulation process is more complicated than for the tonal FSK scheme; in return, the probability of error performance on slowly fading channels is better.
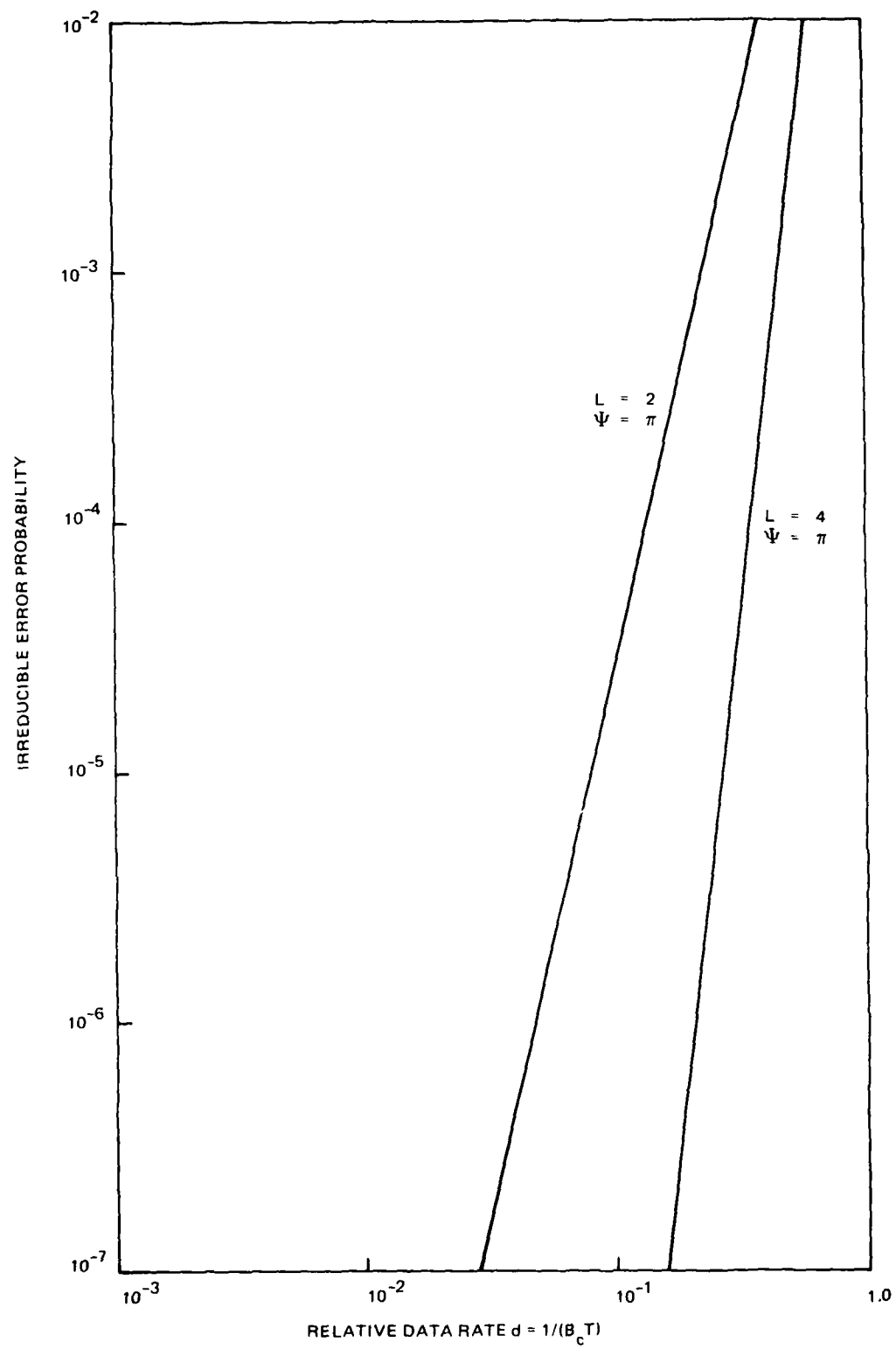
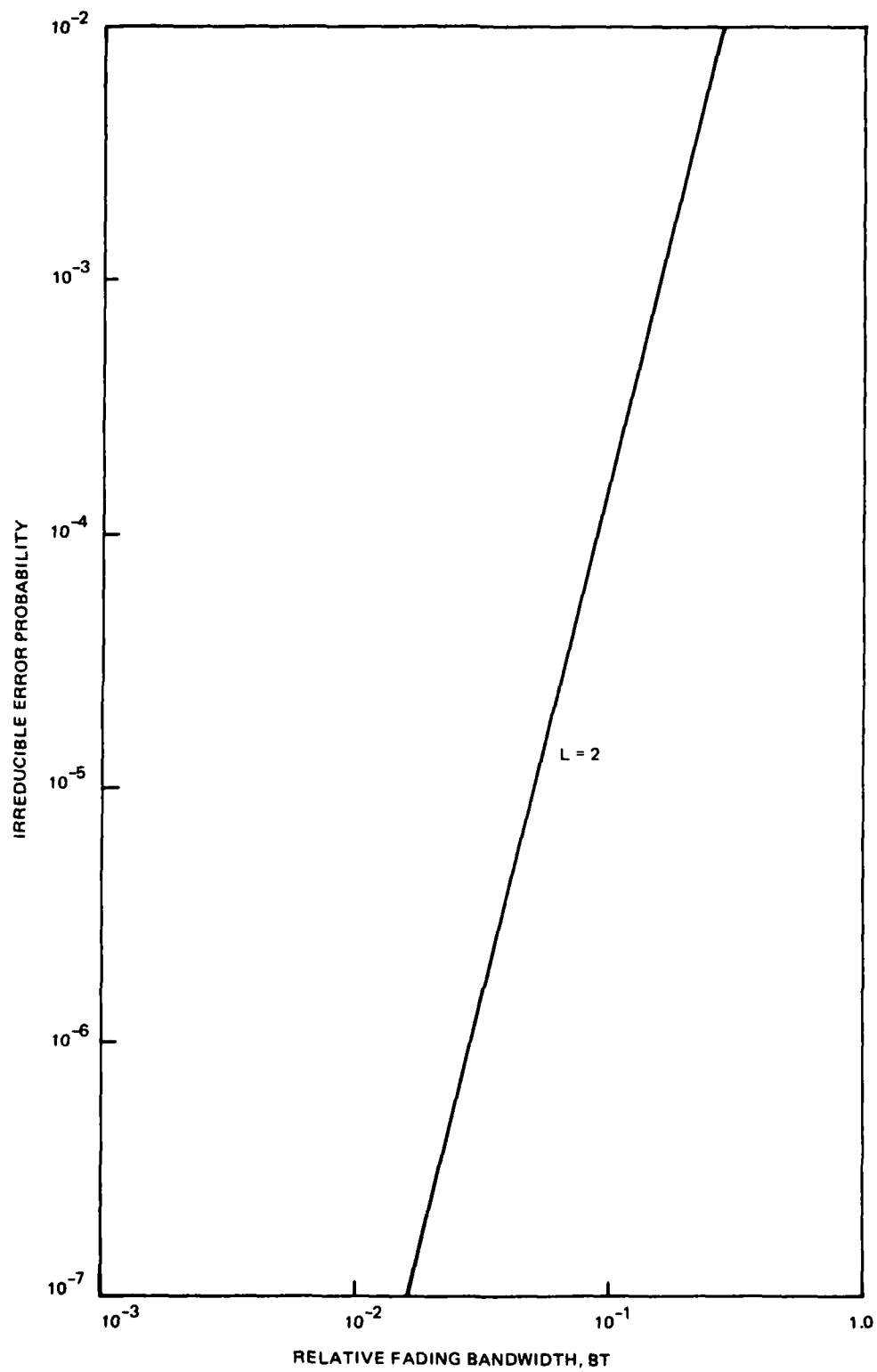Figure 19. Channel with severe time dispersion.

Figure 20. Channel with severe frequency dispersion.

29

There are several ways to modulate spread spectrum signals. For example, the information could be differentially encoded by changing the relative phase from one spread spectrum pulse to the next; this is called differential phase shift key (DPSK). Another approach is to use two independent pseudonoise sequences - one each for mark and space pulses – that may change with time. This is called code shift key (CSK). The technique we examine is frequency shift key (FSK), where the center frequency for the spread spectrum pulse is shifted to one of two frequencies for mark or space. The difference between this scheme and the tonal scheme lies in the spread spectrum modulation and the signal processing at the receiver.

The signal is demodulated by an adaptive signal processing technique that combines the multipath coherently. This scheme is commonly called RAKE (ref 2), after the original system to implement the concept, even though the adaptive techniques now employed may be different.

In essence, in the RAKE technique the receiver measures the channel response by using previous symbols and filters the current symbol through a filter adaptively matched to it. Although the wideband modulation is useful in measuring the channel response, the concept in principle can be applied to any signal format. The crux of the technique lies in matched filtering of the channel output so that the multipath echoes are coherently combined.

Figure 21 is a block diagram for one branch of a RAKE FSK receiver. The receiver adaptively estimates what the received signal will look like, using past symbols, and cross correlates the estimates with the received data to obtain the test statistic J_m. for the mark branch. Similarly the space branch of the receiver produces the test statistic J_s. The receiver decides that a mark is present if

$$q = J_m - J_s > 0 ,$$ (40)

and decides that a space is present if $q \leqslant 0$.

In figure 22A we have sketched an envelope of a spread spectrum signal with symbols of duration T. On the envelope we have marked off two time intervals for decision making and channel estimation. Since the pulse duration (T) is much longer than the anticipated multipath time spread, the decision interval is just the symbol duration, T. The channel pulse response estimation interval, on the other hand, may be longer or shorter than T. Long estimation intervals allow the integration of more signal energy, with the result that a more reliable channel estimate is developed. However, if the channel rate of change is high (commensurate with $1/T$), we will want to make T_e very short so that we obtain a valid estimate of the channel for the information interval.

The dynamics of the RAKE technique make mathematical analysis of it very difficult. Our approach is to reduce to their fundamentals the signal structure and processing and to evaluate a simpler but informative problem. Figure 22B is a simplified signal structure in which we consider only one pair of decision and estimation intervals and ignore the rest of the signal. The signal during the estimation interval is assumed to be known exactly and is called a probe. For our analysis, the probe consists of a mark pulse and a simultaneous space pulse. An adaptive RAKE receiver examines the history of past mark and space symbols to make the channel measurements. The simplification made here is that (1) we guarantee that
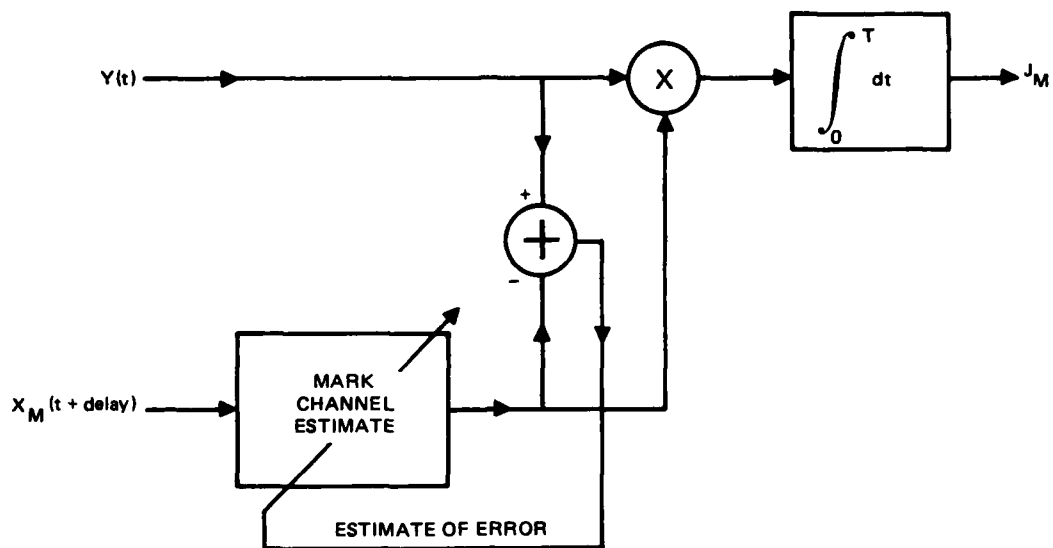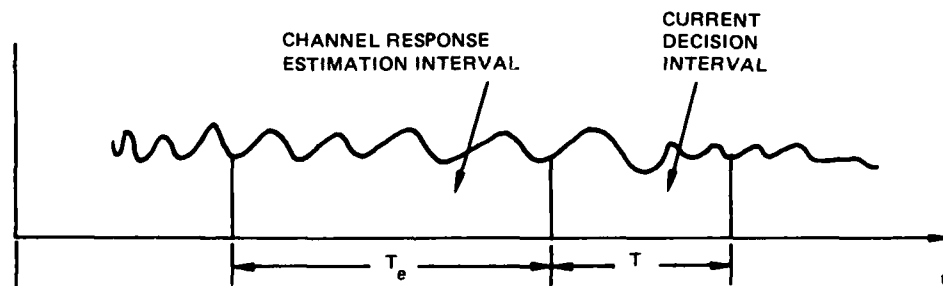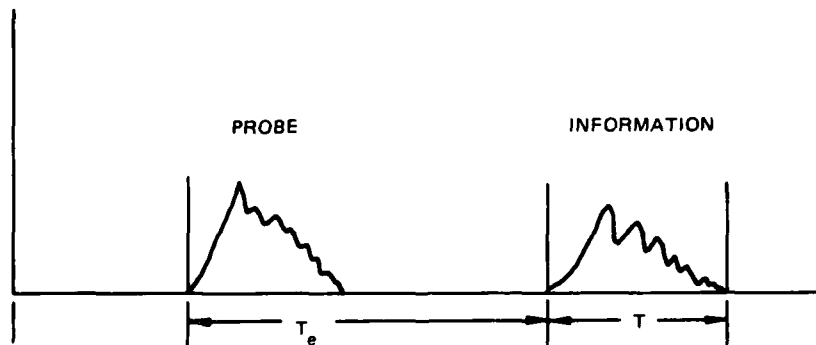
Figure 21. Mark branch of RAKE receiver.

A—DECISION AND ESTIMATION INTERVALS FOR
AN ADAPTIVE PROCESSING RECEIVER

B—SIMPLIFIED MODEL OF DECISION AND ESTIMATION
INTERVALS FOR CHANNELS WITH PULSE RESPONSE
T SECONDS.

Figure 22. Decision and estimation intervals for RAKE analysis.

31

the previous two symbols were a mark and a space, (2) only these two symbols are examined, and (3) they occur together with no penalty to either for additional ageing. This simplified signaling scheme retains the salient feature of the RAKE scheme: (1) The pulses resolve the multipath. (2) The receiver estimates the channel response. (3) The channel response estimate is used to process the information signal adaptively.

In contrast to the tonal FSK, the probe and information signals have large bandwidths and tend to resolve most of the multipath. The signals assumed here are simple pulses with durations much less than T_L. However, the estimation and information decision intervals will be set to T_L seconds, which is the minimum that can be used for measuring the full channel response. As with tonal FSK, we avoid intersymbol interference by restricting our data rate. In this case, however, the bit rate is $1/T_L$ rather than $1/T$, where $T \gg T_L$.

For this simplified model, Hoff (ref 3) has derived the optimum receiver statistics and calculated the probability of error for various channels and values of signal-to-noise ratio, and this was used in what follows. To distinguish the receiver for the simplified model from the traditional RAKE receiver, we refer to it as the probe receiver.

One branch of the probe receiver is shown in figure 23, where $X_0(f)$ and $X_m(f)$ are the Fourier transforms of the probe and information waveforms. $Y_0(t)$ and $Y_1(t)$ are the received probe and information waveforms. Compare figure 23 to the RAKE receiver in figure 21. The optimum receiver is made up of three components: an incoherent detector, a cross correlation detector, and a bias term; whereas the RAKE receiver consists only of a cross correlation detector. On highly time-variant channels, the cross correlation may be poor since the channel response changes (ages) between the time of measurement and the information interval. But the incoherent detector measures the energy only in the two channels, which may be sufficient to distinguish the mark from the space even on highly
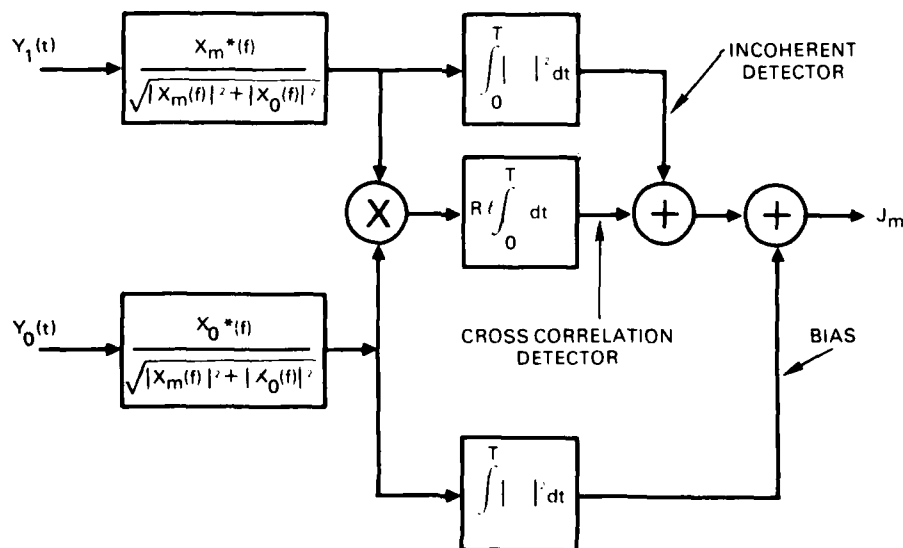

Figure 23. Mark branch of probe receiver.

time-variant channels. The bias term adjusts the mark and space statistics to account for unequal fading on the mark and space channels. In general, the bias is important and should be retained.

The probability of error analysis based upon the simplified model and probe receiver is made in two steps. First we show how RAKE-FSK signaling compares to tonal FSK for multipath time-invariant channels. Second we study the effects of time variance and show how the probability of error degrades with increasing fade rate and Doppler.

Figure 24 compares the probability of error performance for a time-invariant channel for tonal FSK, RAKE-FSK with long pulses, and RAKE-FSK with short pulses. The short pulses are assumed to resolve the multipath. If three multipaths are present, the RAKE-FSK system with short pulses requires about 23 dB less signal-to-noise ratio than tonal FSK to achieve a 10^{-4} bit error rate.

Figure 25 compares the implicit diversity of RAKE-FSK signaling to tonal FSK with diversity. Optimum ratio combining has been chosen for comparison. The probability of error (ref 16, p 533) for L-order diversity is given by the equation

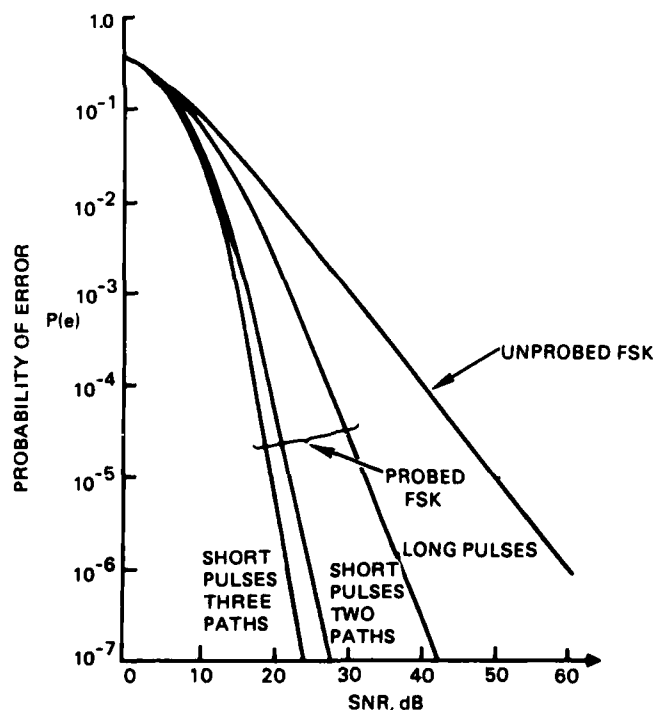$$P(e) = p^L \sum_{j=0}^{L-1} \left(\frac{L+j-1}{j} \right) (1-p)^j , \qquad (41)$$

Figure 24. Probability of error for RAKE signaling on time-invariant channels.

16. J Wozencraft and I Jacobs, Principles of Communication Engineering, John Wiley and Sons, New York, 1965.
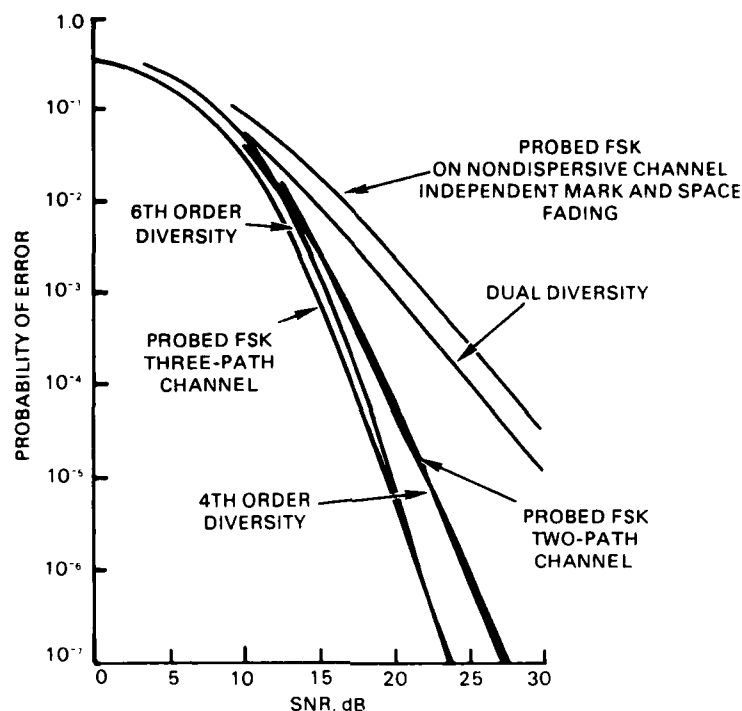
*Figure 25. Comparison of probed FSK signaling and maximum-ratio
diversity combining. The probed FSK originals are short enough to
resolve the multipath.*

where

$$p = \frac{1}{2 + \bar{E}_b/(NL)}$$ (42)

The definition of SNR is the ratio of the average energy per bit to the noise density:

$$SNR = \bar{E}_b/N .$$ (43)

This is the same definition of SNR that is used in the RAKE-FSK signaling analysis. On channels with L equal-strength paths, the RAKE-FSK system can achieve a probability of error comparable to that in a 2L-order diversity system by using pulses that are short compared to the multipath spacing (ref 17).

Time variance is caused by fading and Doppler. In our model, fading and Doppler are specified in hertz by the channel spread (B) and Doppler shift (ν). Our approach to understanding the effect of time variance is to study the behavior of the probability of error for fading and Doppler separately. Figures 26–29 are for two-path channels with either pure

17. GL Turin, Communication Through Noisy, Random-Multipath Channels, IRE Convention Record Part 4, p 154-166, 1956.
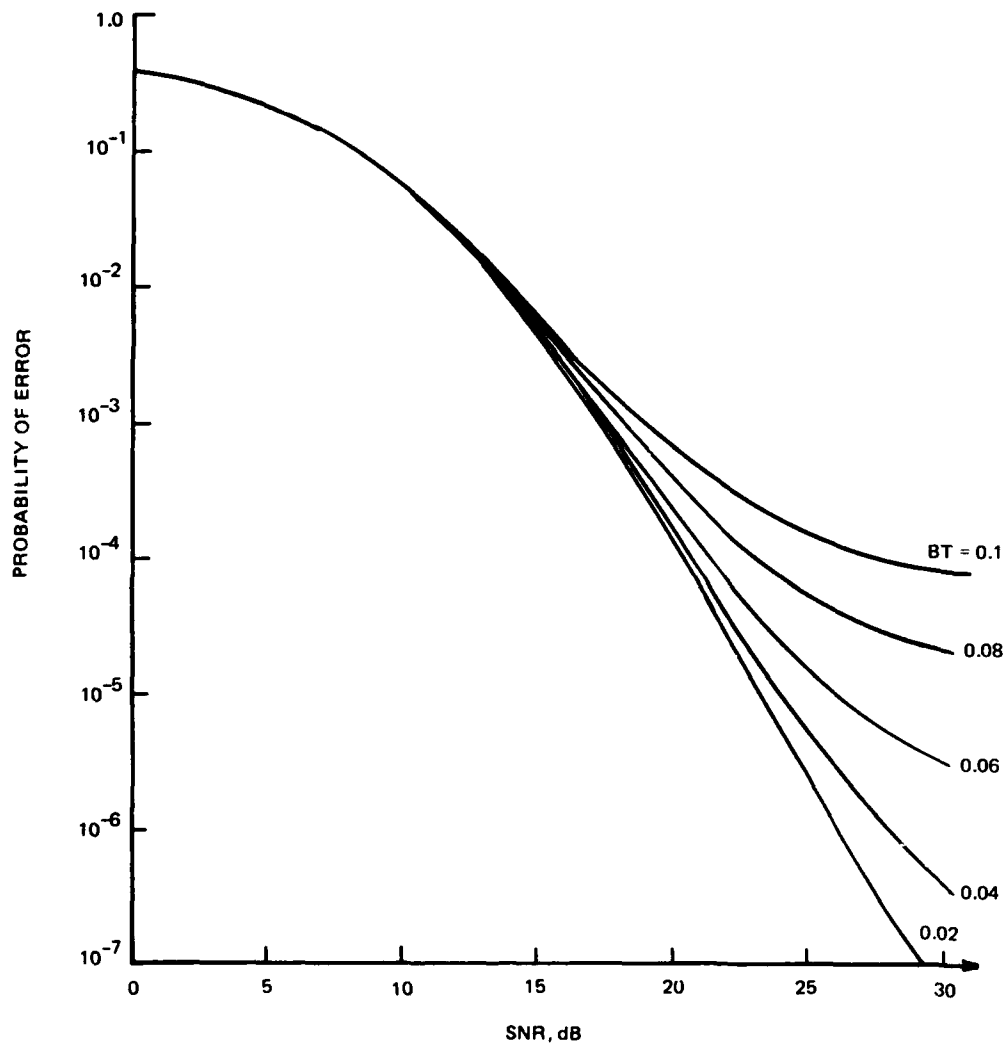
34

Figure 26. Probability of error for standard two-path channel with pure fading.
Channel-spread to pulse-width ratio set to 1.0. Curves parametric in frequency
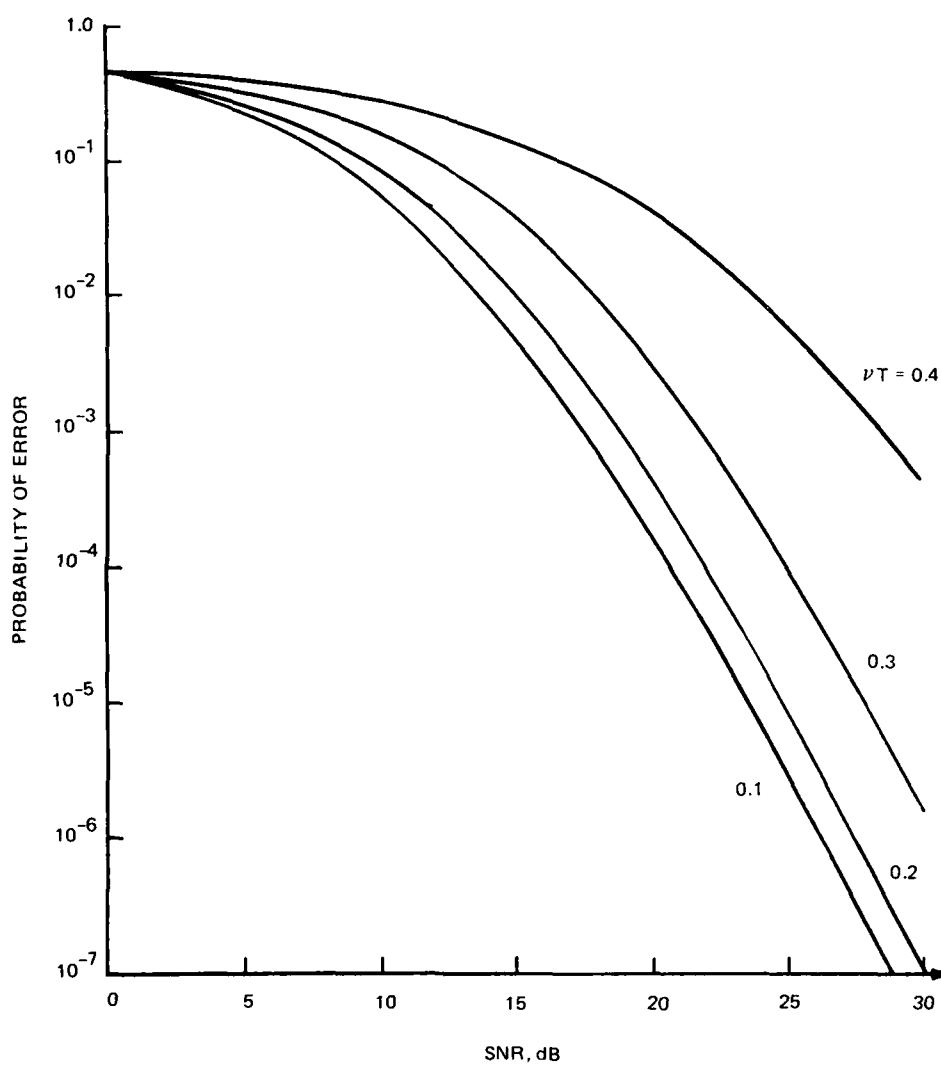spread-time separation product (BT).

Figure 27. Probability of error for standard two-path channel with pure Doppler. Channel-spread to pulse-width ratio set to 1.0. Curves parametric in the Doppler-time-separation product (νT).
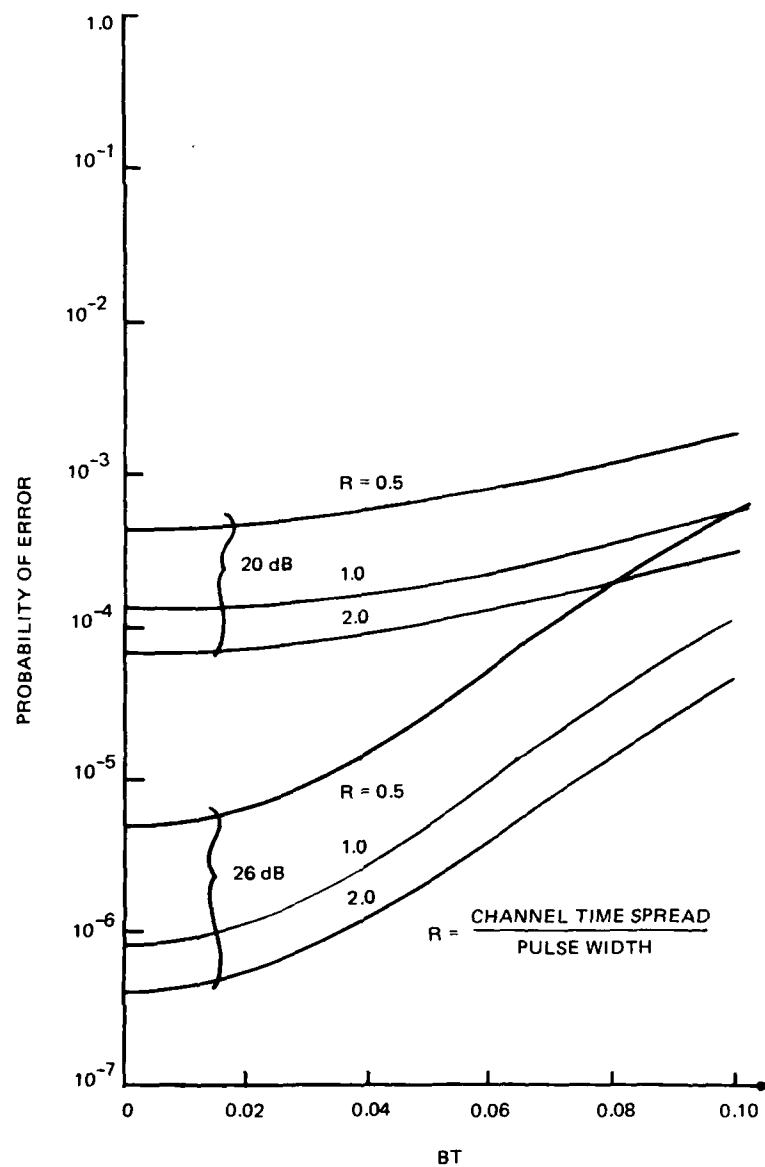
Figure 28. Probability of error versus frequency-spread decision-interval product for standard two-path channel. SNR fixed at 20 and 26 dB.
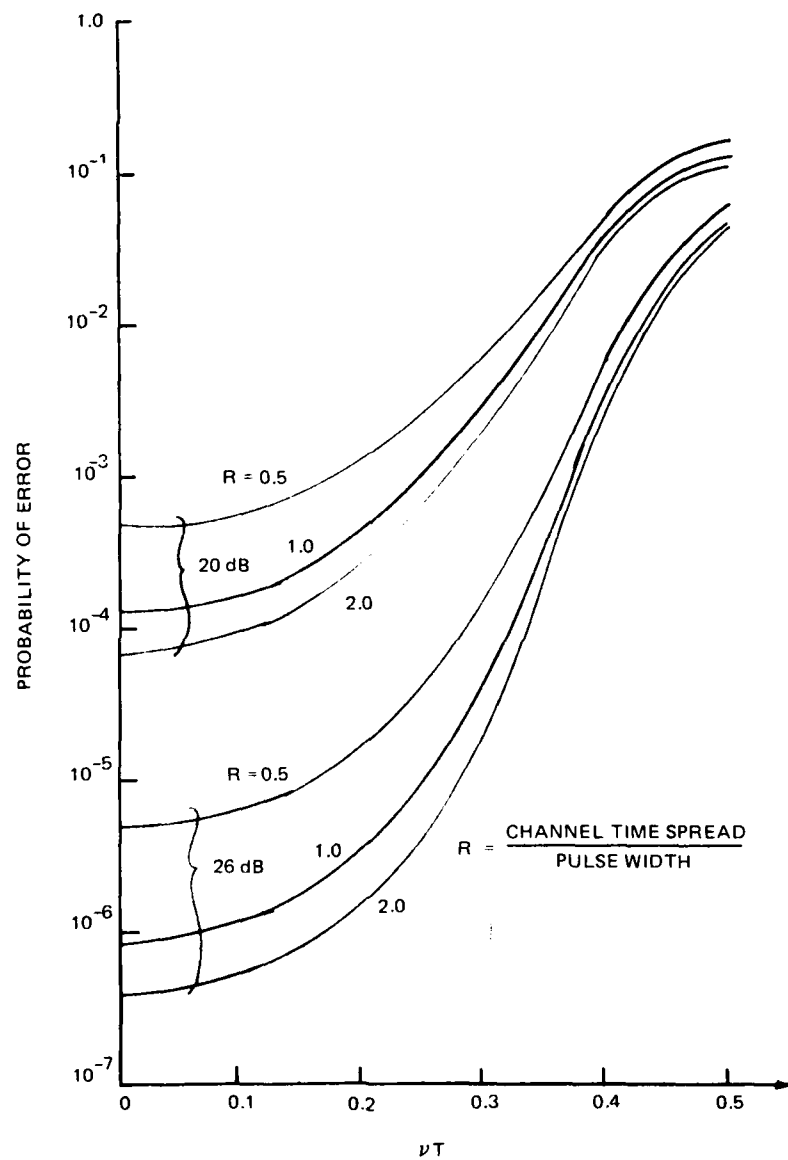
Figure 29. Probability of error versus Doppler decision-interval product for standard two-path channel. SNR fixed at 20 and 26 dB.

38

fading (no Doppler) or pure Doppler (no fading). The fading and Doppler have been normalized by the ageing time between the estimated interval and the decision interval. For the purpose of this analysis, the ageing time is the interval required to make an estimate, which we have set equal to the decision interval (T).

Figure 26 gives the probability of error versus signal-to-noise ratio for a purely fading channel. This example assumes that the pulse width equals the multipath separation, so that the pulse width can just resolve the multipath. The fading results in an irreducible error rate. The faster the fading (B), the higher the irreducible error rate. Fast fading causes the channel to age in the time period between the channel measurement (probe) epoch and the information epoch. The cross correlation in figure 23 becomes very noisy because the channel responses of the probe and information pulses are dissimilar. This noise is present even if the channel additive Gaussian noise is reduced to zero; thus an irreducible error bound exists.

Figure 27 shows the probability of error for a purely Doppler-shifted channel. The higher the Doppler, the higher the error rate. Unlike the purely fading channel, the purely Doppler channel causes the error rate to be higher for all signal-to-noise ratios but does not produce an irreducible error bound. Doppler shift changes the phase relationship between the channel responses of the probe and information epochs. The phase shift reduces the value of the cross correlation term and in some cases can make the term negative. The phase shift does not cause an irreducible error rate, because the incoherent detector can make up for the negative component from the correlator detector by increasing the SNR.

Figures 28 and 29 show how the probability of error increases with fade rate (B) or Doppler shift. The figures show a family of curves that are parametric in the resolution factor (R), given by the relationship

$$R = \frac{\text{channel time spread}}{\text{pulse width}} .$$

The higher the resolution, the lower the error rate. Thus wideband spread spectrum signals are definitely an advantage.

Figure 28 for RAKE signaling is similar to figure 20 for the tonal FSK. The results are not directly comparable however, because the two techniques utilize different signal-to-noise ratios, bit periods (T), and channel conditions. Figures 30 and 31 show how the techniques differ under comparable conditions. In figure 30 we assume that the tonal FSK system uses a bit period (T) that is ten times the multipath spread and that the probe signaling uses a bit decision interval of T_L seconds. The four curves compare the RAKE and tonal FSK signaling schemes at 20 and 30 dB signal-to-noise ratios. For slowly fading channels the RAKE signaling scheme is considerably better than the tonal FSK scheme even though the data rate is higher by a factor of 5. The error rates for both schemes increase as the fade rate (B) increases for a fixed T_L, but the probe signaling scheme can stand a higher fade rate. A possible explanation is that the RAKE signaling scheme uses a shorter bit decision interval (T) than the tonal FSK.

Figure 31 compares the two schemes for equal data rates. Here both systems use a bit decision interval (T) equal to T_L. To do this, we have shortened the tonal FSK signal to $2T_L$ seconds and we use only the middle T_L seconds of the received pulse. The tonal FSK scheme can now withstand higher fade rates at the expense of poorer performance at lower fade rates. Figure 31 suggests that for the two-path channel with fast fading, RAKE-FSK is about 10 dB better than tonal FSK.
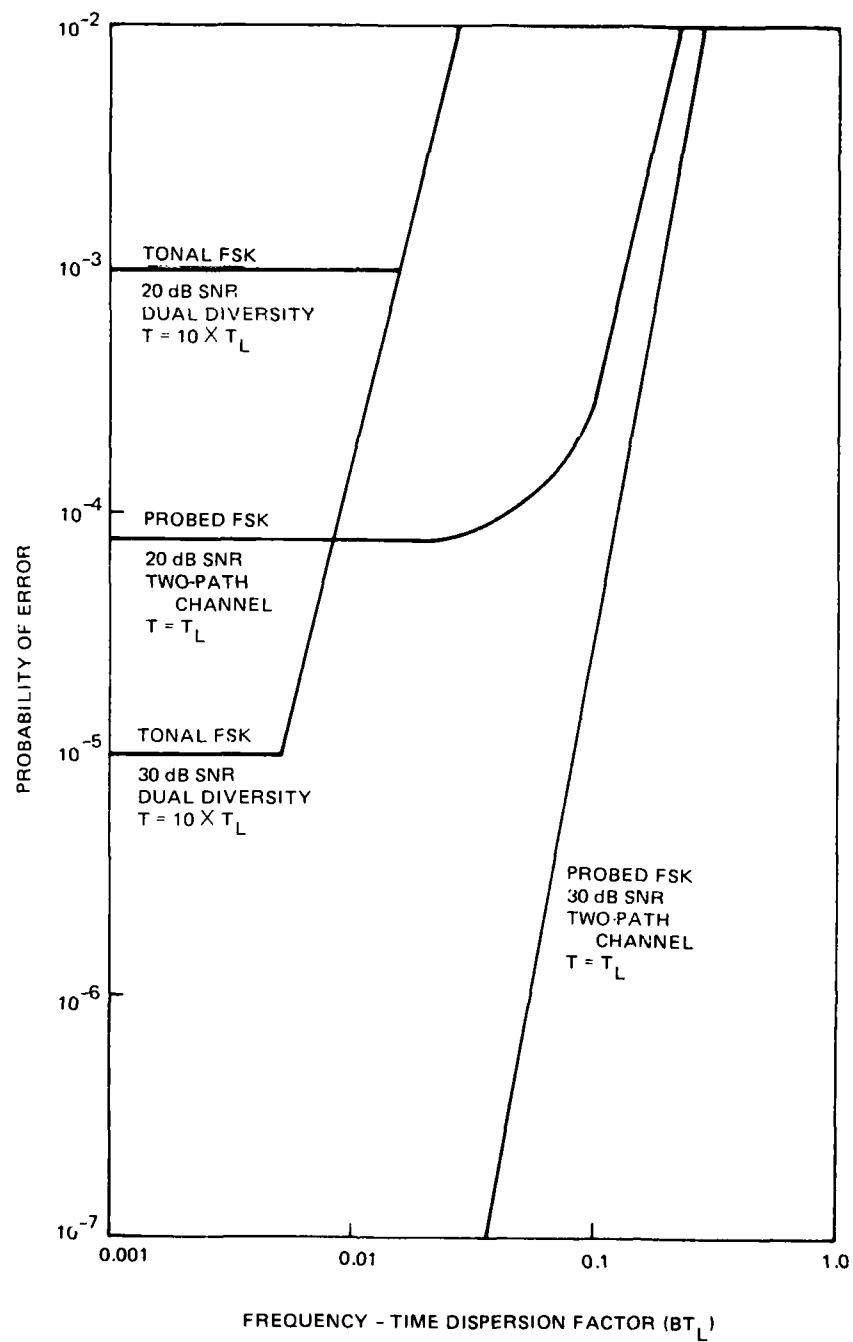
Figure 30. Probability of error comparison of tonal FSK and RAKE-FSK with unequal decision intervals.
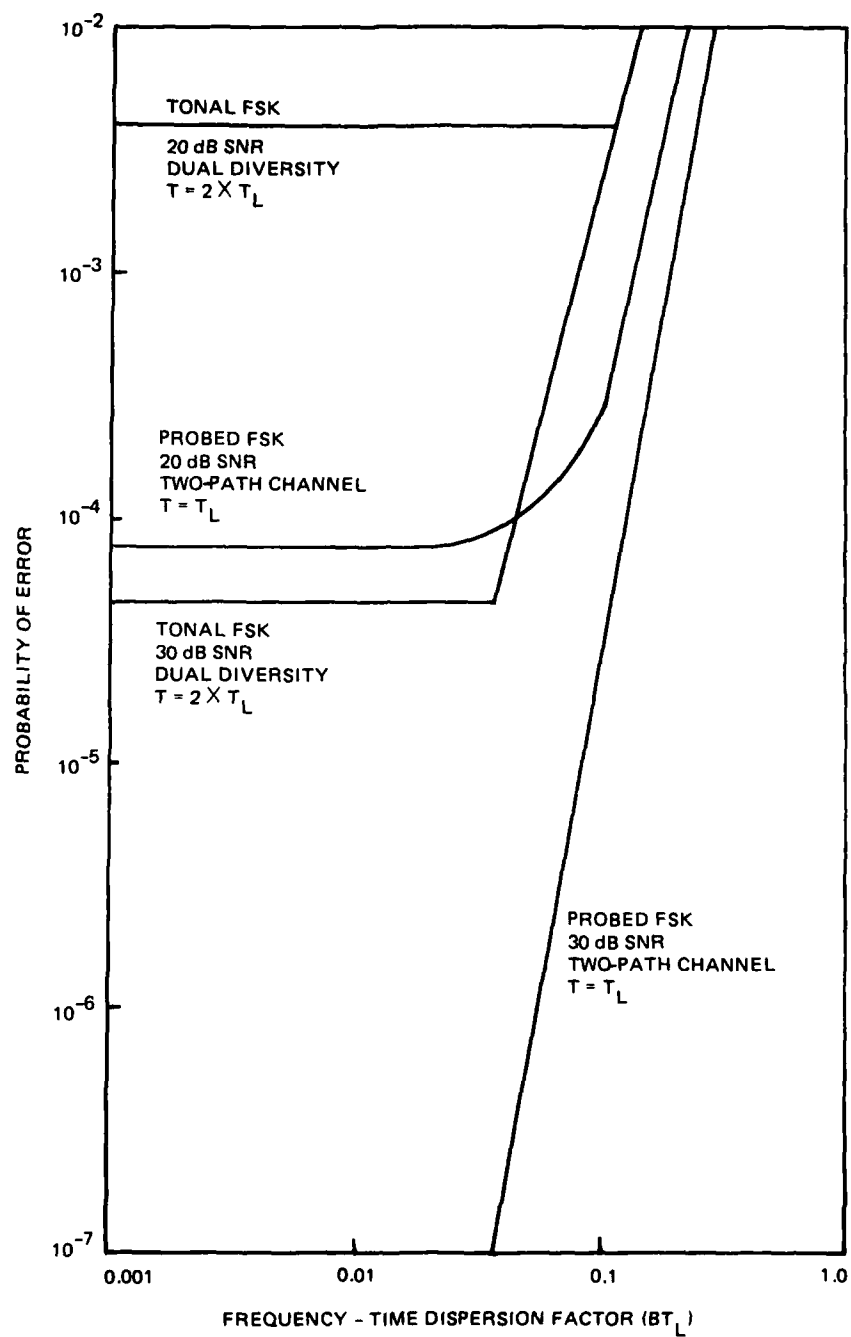
40

Figure 31. Probability of error comparison of tonal FSK and RAKE-FSK with equal decision intervals and data rates.

41

4. CONCLUSIONS

In this report, two mathematical models—a wideband and a narrowband model—have been derived for the underwater acoustic channel. The wideband model is the more general of the two and can characterize channels with large signal bandwidths and severe Doppler distortion. But since the statistics for this model are nonstationary, the application of this model to communication analysis is extremely difficult. The narrowband model has stationary statistics and is derived from the general model by restricting the signals to have bandwidths less than the transmitted center frequency and by restricting the channels to have only minor Doppler shifts. The narrowband model is mathematically similar to hf channel models. Therefore there exists a subset of underwater acoustic channels that are analogous to hf channels but have different scale factors for time and frequency. This fact allows us to extend existing communication performance analysis for RAKE-FSK and tonal FSK from hf channels to a subset of the underwater acoustic channels.

Two signaling schemes are evaluated by using the mathematical results of Bello and Nelin on tonal FSK and the results of Hoff on RAKE signaling. The analysis shows that time variance of the channel causes an irreducible error bound for both signaling schemes. The maximum channel frequency spread (B) that can be tolerated is different for the two schemes and depends upon the receiver decision interval. The RAKE scheme can use a smaller decision interval and can therefore tolerate higher fade rates than the tonal scheme. For very slowly fading channels, the RAKE scheme performs considerably better than the tonal scheme. For example, if three multipaths are present, the tonal system requires a signal-to-noise ratio about 23 dB greater than that required by the RAKE system to achieve a 10^{-4} bit error rate. For the fast-fading two-path channel, the RAKE-FSK scheme is about 10 dB better than tonal FSK at the same data rate.

5. RECOMMENDATIONS

1. Develop an underwater acoustic channel model and verify its accuracy experimentally. Establish a data base of parameters to support the model. Develop a simulation capability based upon the model and the parameter data base.

2. Extend the tonal FSK and RAKE signaling comparison to acoustic channels, where Doppler shifts restrict the channel correlation bandwidth and distort the received signal envelope.

REFERENCES

1.   PA Bello and BD Nelin, The Effect of Frequency Selective Fading on the Binary Error Probabilities of Incoherent And Differentially Coherent Matched Filter Receivers, IEEE Transactions on Communication Systems, p 170-186, June 1963.

2.   R Price and PE Green, Jr, Communication Techniques For Multipath Channels, Proceedings of the IRE, vol 46, p 555-570, March 1958.

3. LE Hoff, Probe Signaling on Fading Multipath Communication Channels, PhD thesis at the University of California, San Diego, 1979.

4. CB Officer, Sound Transmission, McGraw-Hill Book Company Inc, New York, 1958, chapter 4.

5. I Tolstoy and CS Clay, Ocean Acoustics, McGraw-Hill Book Company, New York, 1966, chapter 5.

6. RJ Urich, Multipath Propagation and Its Effects on Sonar Design and Performance in the Real Ocean, paper in Aspects of Signal Processing, Part I, edited by G Taccone; D Reidel Publishing Company, 1977.

7. RL Veenkant, Investigation of the Propagation Stability of a Doubly Spread Underwater Acoustic Channel, IEEE Transactions on Acoustics, Speech and Signal Processing, vol ASSP-25, no 2, April 1977.

8. RD Chapman, Sound Scattering in the Ocean, vol 2, p 161 of Underwater Acoustics, edited by VM Albers, Plenum Press, New York, 1967.

9. J Johnsen, Models of the Underwater Acoustic Channel, Eighth International Congress on Acoustics, London, 1974.

10. C Helstrom, Statistical Theory of Signal Detection, Pergamon, Second Edition, Oxford, 1968.

11. M Schwartz, WR Bennett, and S Stein, Communication Systems and Techniques, McGraw-Hill Book Company, New York, 1966.

12. CC Watterson, J Juroshek, and W Bensema, Experimental Confirmation of an HF Channel Model, IEEE Transactions on Communication Technology, vol 18, no 6, p 792-803, December 1970.

13. PA Bello and BD Nelin, The Influence of Fading Spectrum on the Binary Error Probabilities of Incoherent and Differentially Coherent Matched Filter Receiver, IRE Transactions on Communication Systems, p 160-168, June 1962.

14. PM Hahn, Theoretical Diversity Improvement in Multiple Frequency Shift Keying, IRE Transactions on Communication Systems, p 117-184, June 1962.

15. RF Daly, Analysis of Multipath Effects on FSK Error Probability for a Simple HF Channel Model, Stanford Research Institute Memorandum 1, Project 4554 Control SD-189, Office of Secretary of Defense, Washington, DC, February 1964.

16. J Wozencraft and I Jacobs, Principles of Communication Engineering, John Wiley and Sons, New York, 1965.

17. GL Turin, Communication Through Noisy, Random-Multipath Channels, IRE Convention Record Part 4, p 154-166, 1956.

DISTRIBUTION LIST

CHIEF OF NAVAL RESEARCH
    CODE 100 (RADM LEONARD KOLLMORGEN)

NAVAL ELECTRONIC SYSTEMS COMMAND
    PME 611A (TB HUGHES)   (3)
    PME 110-3 (RM DYSON)

NAVAL SEA SYSTEMS COMMAND
    CODE 06HI (C SMITH)
    CODE 06HI (DG HOFFMAN)

NAVAL RESEARCH LABORATORY
    CODE 5144 (AA GERLACH)

NAVAL UNDERWATER SYSTEMS CENTER
    NEW LONDON LABORATORY
    CODE 3292 (AW ELLINTHROPE)

UNIVERSITY OF CALIFORNIA – LOS ANGELES
ELECTRONIC ENGINEERING DEPARTMENT
405 HILGARD AVENUE
LOS ANGELES, CA 90024
    J OMURA

UNIVERSITY OF CALIFORNIA – SAN DIEGO
ELECTRICAL ENGINEERING/COMPUTER SCIENCE
    DEPARTMENT
LA JOLLA, CA 92093
    R LUGANNANI
    C HELSTROM

UNIVERSITY OF MIAMI
DEPARTMENT OF ELECTRICAL ENGINEERING
UNIVERSITY STATION
CORAL GABLES, FL 33124
    CV KIMBALL

UNIVERSITY OF MICHIGAN
COOLEY ELECTRONICS LABORATORY
ANN ARBOR, MI 48104
    T. BIRDSALL

DYNAMICS TECHNOLOGY, INC.
22939 HAWTHORNE BLVD.
TORRANCE, CA 90505
    G DONAHUE
    E SATORIUS

RAYTHEON COMPANY
PO BOX 360
WEST MAIN ROAD
PORTSMOUTH, RI 02871
    WC KNIGHT

RCA
FRONT AND COOPER STREETS
MAIL STOP 10-7-7
CAMDEN, NJ 08102
    P REED

SIGNATRON, INC.
12 HARTWELL AVENUE
LEXINGTON, MA 02173
    JN PIERCE
    P MONSEN

STEIN AND ASSOCIATES
280 DAY HILL
WALTHAM, MA 02154
    S STEIN

TEXAS INSTRUMENTS
PO BOX 225012
MAIL STATION 234
DALLAS, TX 75265
    D HYDE

TRACOR
9797 AERO DRIVE
SAN DIEGO, CA 92123
    WJ JAY

DEFENSE TECHNICAL INFORMATION CENTER (12)

DATE
ILME